(1)

SELECTIVE EXCITATION LUMINESCENCE AND PHOTOLUMINESCENCE INVESTIGATIONS OF YTTERBIUM DOPED InP, GaAs AND AlGaAs

THESIS

Michael L. Eastman
Captain, USAF
AFIT/GEP/ENP/89D-3

DEPARTMENT OF THE AIR FORCE
AIR UNIVERSITY
AIR FORCE INSTITUTE OF TECHNOLOGY

Wright-Patterson Air Force Base, Ohio

AFIT/GEP/ENP/89D-3

SELECTIVE EXCITATION LUMINESCENCE AND PHOTOLUMINESCENCE INVESTIGATIONS OF YTTERBIUM DOPED InP, GaAs AND AlGaAs

THESIS

Michael L. Eastman
Captain, USAF
AFIT/GEP/ENP/89D-3

AFIT/GEP/ENP/89D-3

SELECTIVE EXCITATION LUMINESCENCE AND PHOTOLUMINESCENCE INVESTIGATIONS OF YTTERBIUM DOPED InP, GaAs AND AlGaAs

THESIS

Presented to the Faculty of the School of Engineering
of the Air Force Institute of Technology
Air University
In Partial Fulfillment of the
Requirements for the Degree of
Master of Science in Engineering Physics

Michael L. Eastman, B.S.
Captain, USAF

December 1989

Acknowledgements

The completion of this research project leaves me indebted to several people. I thank my advisers, Dr. Yung Kee Yeo and Dr. Robert L. Hengehold, for their guidance and suggestions. Many thanks, indeed, go to Jose Colon and Gernot S. Pomrenke for their countless pieces of valuable information and to Greg Smith, laboratory technician, for all of his technical assistance during endless equipment failures.

I owe much to my family, Barb, Jason, Kristi, and the new one, Jeffrey, born in October. They have been tremendous supports during this difficult program. My goal now is to convince them I love them as much as they think I love the PC.

Michael L. Eastman

Table of Contents

List of Figures

Abstract

Group III-V semiconductors doped with rare earth (RE) elements produce sharp emissions that would be ideally suited to Air Force optoelectronic applications. The sharp emissions are due to the intra-4f transitions of the triply ionized RE atom that are partially shielded from the crystal lattice potential by the outer lying 5s and 5p electrons. In this work the RE element ytterbium (Yb) was implanted into bulk grown InP, vapor phase epitaxial (VPE) grown InP, GaAs, and $Al_xGa_{1-x}As$ with x = .15, .23 and .30. The Yb was implanted at 1 MeV at a dosage of $3 \times 10^{13}/cm^2$. The samples were annealed using rapid thermal annealing (RTA) or conventional furnace annealing (CFA) for a range of temperatures and times.

The study of bulk InP:Yb evaluated the emission spectra intensity as a function of temperature and excitation energy. Temperatures from 2.8K to 90K and energies from 1.38 eV to 1.495 eV were used. The results of this analysis confirm that the majority of the Yb related spectra is from only one luminescent center. They also illustrate a definite peak in emission intensity at excitation energies that correlate to the excitonic absorption region of the semiconductor. This indicates that the excitons and/or free carriers are required for the transfer of energy to the Yb ions. An incident power versus line intensity study was

a. . accomplished. Results indicate most lines saturate at higher powers but the 1.248 eV line (line 2) increases significantly, possibly as a result of its "hot line" characteristic.

The study of VPE InP:Yb involved excitation over a narrow range that corresponds to the band edge. Donor-acceptor (D^{o},A^{o}) pair transitions were monitored as well as Yb emissions. Results showed a substantial dip in the (D^{o},A^{o}) emissions with a simultaneous minor peak in the Yb signal. Although this seems to indicate a possible link between (D^{o},A^{o}) transfer of energy to Yb, the slight change in Yb intensity indicates that if this is a transfer method, it is extremely inefficient.

The photoluminescence of many GaAs:Yb and AlGaAs:Yb samples were examined but no characteristic Yb emissions were found. Some of the samples had previously been studied and had exhibited very weak Yb related signals. The possibility of signal quenching by storage and annealing is proposed.

SELECTIVE EXCITATION LUMINESCENCE AND PHOTOLUMINESCENCE INVESTIGATIONS OF YTTERBIUM DOPED InP, GaAs, AND AlGaAs

Introduction

Over the last decade rare-earth (RE) doped III-V semiconductors have gained considerable attention from physicists and engineers around the world. Although the luminescent properties of RE 4f transitions have been studied for many years, they have been primarily embedded in host solids of dominantly ionic bond character, such as halides and oxides. Perhaps due to the low solubility of RE's in dominantly covalent hosts and their notorious affinity to oxygen contaminations, the study of lanthanide doped III-V semiconductors has been started only recently (1). The intense, extremely sharp emissions of the 4f-4f transitions of the rare earth ions make them prime candidates for widespread optoelectronic and photonic applications, which is the primary incentive for Air Force participation in this research. Since fiber optic cables have their least dispersion and lowest absorption in the 1.3-1.5 μm region, sharp, intense radiation from RE doped semiconductors could vastly improve the efficiency and speed of AF communications systems. Research has already produced

an InP:Yb light emitting diode (LED) and a GaInAsP:Er semiconductor injection laser (2,3).

Perhaps with such applications in mind Kasatkin et al initiated the in-depth study of the photo- and electro-luminescent properties of RE doped III-V semiconductors that continues today. Their paper, published in 1980, highlighted the photoluminescence spectra that is characteristic of intracenter transitions of the Yb^{3+} impurities in gallium phosphide (GaP) (4). In the subsequent years, the rare earths praseodymium (Pr), neodymium (Nd), samarium (Sm), europium (Eu), gadolinium (Gd), dysprosium (Dy), erbium (Er), and thulium (Tm) doped into various III-V semiconductors have also been investigated to some degree. In 1981, Zakharenkov et al reported on the first photoluminescence of Yb^{3+} ions doped into indium phosphide (InP) (5). Since then it has been recognized to have one of the strongest emissions of the RE's doped into semiconductors. It has been widely studied using photoluminescence (PL), photoluminescence excitation spectroscopy (PLE), Zeeman analysis, paramagnetic resonance, and electron spin resonance.

Although the crystal field's effect on the Yb^{3+} ion is well accepted, there appears to be no definite conclusions drawn concerning the excitation mechanisms of the Yb luminescence. The purpose of this research is to apply selective excitation luminescence (SEL) studies specifically

to deduce the excitation mechanism by which the InP:Yb converts incident laser radiation to intense emissions near 1 μm. This research will also investigate the photoluminescence of GaAs and AlGaAs, applying SEL techniques if appropriate.

The importance of this type of research cannot be over emphasized. The future of the optoelectronic industry is strongly based on III-V semiconductors. If sharp, intense signals can be obtained from RE doped III-V material at room temperature, the Air Force's optoelectronic communications systems could very well be revolutionized by faster and more efficient communications.

Background

Semiconductor Theory

An ideal crystalline lattice is one in which the atoms that make up the solid are regularly and predictably spaced. The atoms are bound together either by covalent, ionic, or metallic binding. In general, group IV elements of the periodic table form covalent bonds such that each atom has four valence electrons with which it "shares" with its four nearest neighbors. The bonds are strongly directional in that the electrons are concentrated along the lines joining the atoms and the lines tend to be disposed tetrahedrally about any atom (6:16). The bonds are typically strong resulting in high melting and boiling points.

Group I-VII compounds form highly ionic bonds in that electrons are transferred from one atom to another. The crystal is thus made up of positively and negatively charged ions and is held together by the electrostatic potential between the ions. The bonds are again fairly strong and the charge distribution of each ion is spherically symmetric.

The metallic elements form metallic crystals in which free electrons are present. It is these free electrons that give metals their characteristic electrical and thermal conductivity. The binding energy arises from the interaction of the free electron "gas" with the positive ions in the lattice. The complexity of the interaction can

result in very low to very high binding energies.

Group II-VI and III-V compounds exhibit both covalent and ionic properties with group III-V compounds more nearly covalent than II-VI compounds. It is the group IV and group III-V compound semiconductors that will be discussed further.

In a given crystal lattice there exists bands of energy that are "forbidden", i.e., electrons may not occupy certain energy bands due to the periodicity of the lattice. At the lowest temperatures all electrons would be at their lowest energy level available. The highest filled band is called the valance band and the next allowed energy band is the conduction band. When the solid is heated some electrons may be thermally excited across the bandgap into the conduction band. Only electrons in the conduction band and holes in the valence band contribute to the electrical conductivity of the material. In an insulator electrons just fill the valence band and the gap between the valence and conduction bands is so great that it is almost impossible to thermally excite the electrons across the gap in anpreciable numbers. Thus, the insulator is a poor conductor.

In metals a band may be only partially filled. In this case, the electrons act as a free electron gas that is free to conduct. Also, in metals two bands may overlap such that thermal excitation causes electrons to spill over into the

next energy level. The result is a large number of electrons that are free to move about (6:246). Finally, if the gap between the valence and conduction bands is relatively narrow when the valence band would be just full at 0K, electrons can fairly easily be thermally excited across the gap in sufficient numbers to increase the conductivity of the material. Again, not only will the new electrons in the conduction band contribute to the conductivity, the empty electronic states (holes) in the valence band also contribute. The conductivity is generally less than that of a metal due to the limited number of electrons; hence, the name "semiconductor".

Impurities in the semiconductor can add energy levels between the conduction and valence bands. These additional energy levels allow electrons to be more easily excited into the conduction band from the impurity or out of the valence band into the impurity. The impurities exist in even the highest quality crystals but can also be intentionally be added to the semiconductor to control its electrical and optical properties. When the semiconductor is "doped" with impurity atoms that have fewer electrons in their outer shell than the atoms of the crystal that they replace, the impurity is called an acceptor. An acceptor's energy level is just slightly above the valence band such that it can easily accept electrons from the crystal lattice, leaving a conducting hole in the valence band. If the impurity atoms

have extra electrons over that required for bonding, they are called donors. The donor energy level lies just below the conduction band, and hence the extra electrons can be easily excited into the conduction band. For either the donor or acceptor impurity the energy required for ionization can be approximated by (6:268)

$$E_{a,d} = 4\pi^2 e^4 m^* / 2K^2 h^2 \quad (1)$$

where e is the electronic charge, m^* is the effective mass of the hole or electron, K is the relative dielectric constant and h is Planck's constant.

Energy levels are also added to the bandgap by the existence of defects and excitons. Defects of crystals have been categorized by many researchers. The primary defects of interest, those associated with the optical properties of a material, are point and chemical defects. Point defects occur in the crystal as atoms out of lattice sites (interstitial defect), and as the absence of atoms at lattice sites (vacancy defect). Chemical defects are those due to impurity atoms in lattice or interstitial positions (7:69). Chemical defects have been discussed in previous paragraphs and their effects on the semiconductor have been explained. Point defects and their effects on this research will be discussed further in later sections.

When an electron in the conduction band and a hole in the valence band are in the vicinity of each other, a Coulomb interaction can occur between them. The electron

and hole will rotate around each other much as in a hydrogen-like atom, and since the covalent crystal's dielectric constant is high, the radius can be fairly large. The electron-hole pair is known as an exciton and has less energy than when the the electron and hole are far apart with the electron in the conduction band (8:81). Therefore, the excitonic energy is just below that of the conduction band and it can be given by (9:12)

$$E_x = - 2\pi^2 \mu e^4 / h^2 K^2 n^2 \tag{2}$$

where μ is the reduced mass of the respective effective masses of the electron and the hole and n is the quantum number describing the exciton state.

The exciton can be free to transport energy through the lattice or it can be bound to an impurity with energy E_b (8:87). Only in extremely pure material will excitons dominate the luminescence spectrum; in less pure samples the impurity effects will dominate. This is due to the high mobility of the free excitons; as the exciton moves through the material, it encounters defects of various kinds and tends to decay in the vicinity of one of these centers (8:84). Excitonic transitions will be further discussed in a later section.

Crystal Growth

Since the invention of the transistor in 1948, the success of solid state devices has been highly dependent on

the ability to grow pure, single crystal semiconductors. Technological advances in this area now allow silicon (Si) growth with concentrations of most impurities of less that one part in ten billion (10:12). Although crystal growth methods for other semiconductors have not reached that level of purity, there is reason to believe that significant advances in technology will be made in the near future.

There are several methods by which high quality crystals are grown. Each technique leads to slightly different purities and performance characteristics. The following paragraphs will briefly introduce several of the methods currently being used in the industry to grow high quality substrates.

The horizontal Bridgeman method of crystal growth involves selective cooling of molten material so that solidification occurs along a specific crystal direction. This can be accomplished by drawing a quartz crucible containing the molten material through a furnace so that solidification begins at one end and proceeds slowly down the length of the bar. A disadvantage to this method is that the molten material is in contact with the sides of the crucible which will induce stress and impurities into the lattice structure. The stress can be reduced by using the Czochralski method which involves lowering a seed crystal into molten material and then drawing it out. As the seed is raised slowly, the crystal is allowed to grow. Single

crystals as large as five inches in diameter have been grown using this method. If the molten material includes a particularly volatile element, i.e., As in GaAs, a dense layer of B_2O_3 may be floated on top of the crystal material to prevent evaporation. This is called liquid-encapsulated Czochralski (LEC) growth (10:14). A drawback to any growth method that requires crystal melting is the addition of impurities from the crucible.

A method used to reduce the addition of impurities during the growth process is liquid phase epitaxy (LPE). LPE allows the growth of a single crystal on a substrate material at a temperature much lower than the crystal's melting temperature (10:19).

Another method that allows high purity epitaxial layer growth on semiconductor or insulator substrates is called vapor phase epitaxy (VPE). The epitaxial layers are grown by controlling the deposition of the desired atoms onto the substrate. For example, an epilayer of Si can be deposited on a substrate in a reaction chamber by the pyrolysis of silane at 1000°C by the reaction:

(3) $$SiH_4 \longrightarrow Si + 2H_2$$

At this temperature, migration of impurities from the substrate to the epilayer is reduced (10:21). A similar method known as metal organic chemical vapor deposition (MOCVD) is useful for growing compound semiconductors. For example, if trimethylgallium is reacted with arsine by

(4) $(CH_3)_3Ga + AsH_3 \rightarrow GaAs + 3CH_4$

at 700°C, the result is a high quality GaAs layer. If trimethylaluminum is added to the mixture in controlled quantity, epilayers of AlGaAs can be grown (10:22).

The highest quality samples can be grown by molecular beam epitaxy (MBE). The substrate is held in a vacuum while molecular or atomic beams of the constituents are directed onto its surface. Over 100 alternating layers of GaAs and AlGaAs have been grown in a space of 3.3 μm by using high speed controlling shutters in the beams of the constituents (10:24).

Impurities can be intentionally added to the substrates or epitaxial layers in a number of ways. They can be added to the melt and bulk grown, grown into an epilayer using VPE, or most commonly, implanted using ion implantation techniques with subsequent annealing. The first two methods are fairly straight forward in consideration of previous paragraphs and will not be further discussed. Ion implantation and annealing will be the topics of the next section.

Ion Implantation and Annealing

An ion implantation accelerator can be used to direct a beam of ions, at very high energy, into the sample. The advantages of ion implantation are that the results are generally reproducible, the dopant profile is well defined, and various profiles are available. The two most common

profiles are the Linhard, Scharff, and Schiott (LSS) calculation and the Pearson type-IV distribution (11:10-56). Figure 1 illustrates a Pearson type-IV distribution for InP:Yb as used in this research.

The primary disadvantage of ion implantation is that it usually damages the crystal by dislocating substrate atoms from lattice sites and by introducing substantial point defects (such as vacancies and interstitial defects) and dislocations. High temperature annealing is used to repair the damage and cause the interstitially located impurities to fall into substitutional sites. Two primary annealing methods are used: 1) conventional furnace annealing (CFA), and 2) rapid thermal annealing (RTA).

CFA is accomplished by placing the sample(s) in an annealing tube with N_2, H_2 or forming gas flowing over the sample. The sample is heated at a desired temperature for a period of 10-15 minutes. During this period, the more volatile atoms in the substrate may dissociate, damaging the surface rather than repairing it. To prevent dissociation a chemical film can be placed on the sample prior to annealing. Another method commonly used is to place an implanted sample face down on an unimplanted substrate of the same crystal type during annealing; this prevents the escape of such atoms as P in InP and GaP, and As in GaAs. This latter technique is known as proximity annealing. Figure 2 illustrates the CFA method.

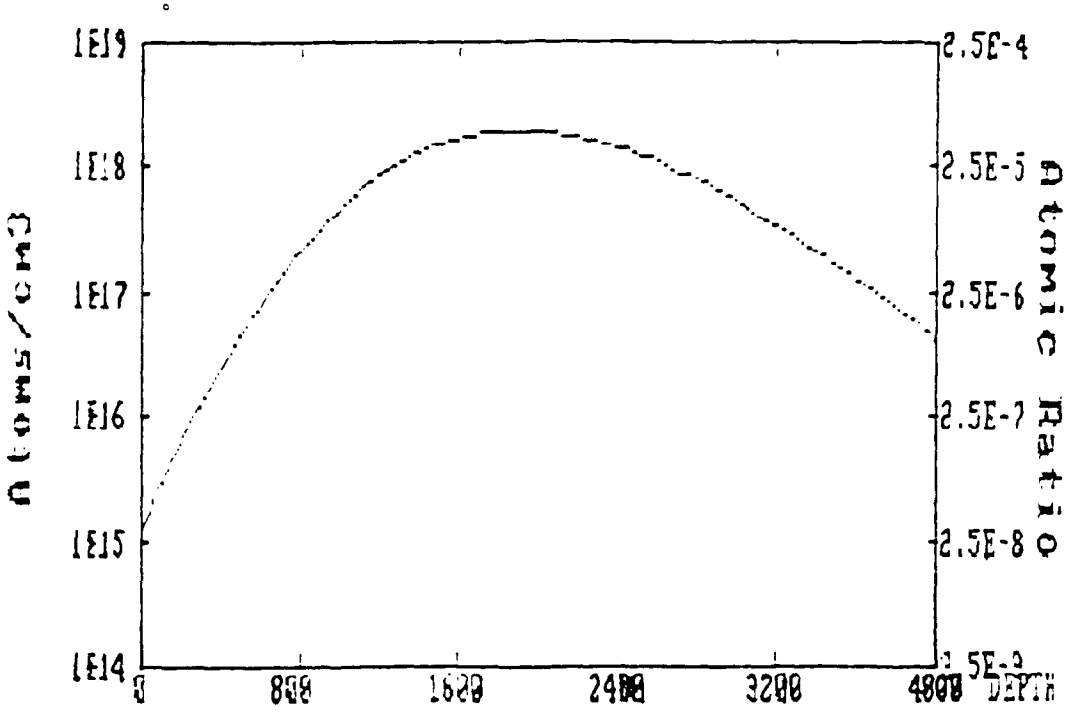

Figure 1. Pearson Distribution of Yb Ions Implanted into InP at 1 MeV with a Dosage of 3 x $10^{13}/cm^2$. ("Profile Computer Code by Implant Sciences Corp., Danvers, Mass.) (Courtesy of Jose E. Colon.)

Unfortunately, the long times required for CFA can cause a redistribution of the dopant profile. The RTA method was developed to alleviate this problem. In this technique the sample is kept thermally isolated and is heated by radiation. This allows accurate control of the heating and cooling rates and allows much shorter annealing time than required for CFA. The RTA method is sketched in Figure 3.

Luminescence

The luminescence of a material can be investigated using several techniques. This section will discuss the luminescent properties and various methods used to examine them.

Photoluminescence.

Photoluminescence is a nondestructive technique used to spectroscopically evaluate the character of semiconductors. A laser of above bandgap energy is generally used to excite the sample; the luminescence of the semiconductor can then be studied using a spectrometer and a suitable detector. Information on the host crystal (intrinsic properties), the impurities and defects (extrinsic properties), and the interaction of the two can be discerned.

Luminescence of the sample is due to the radiative transitions that occur when absorbed energy is released via the emission of photons. The photons have a characteristic

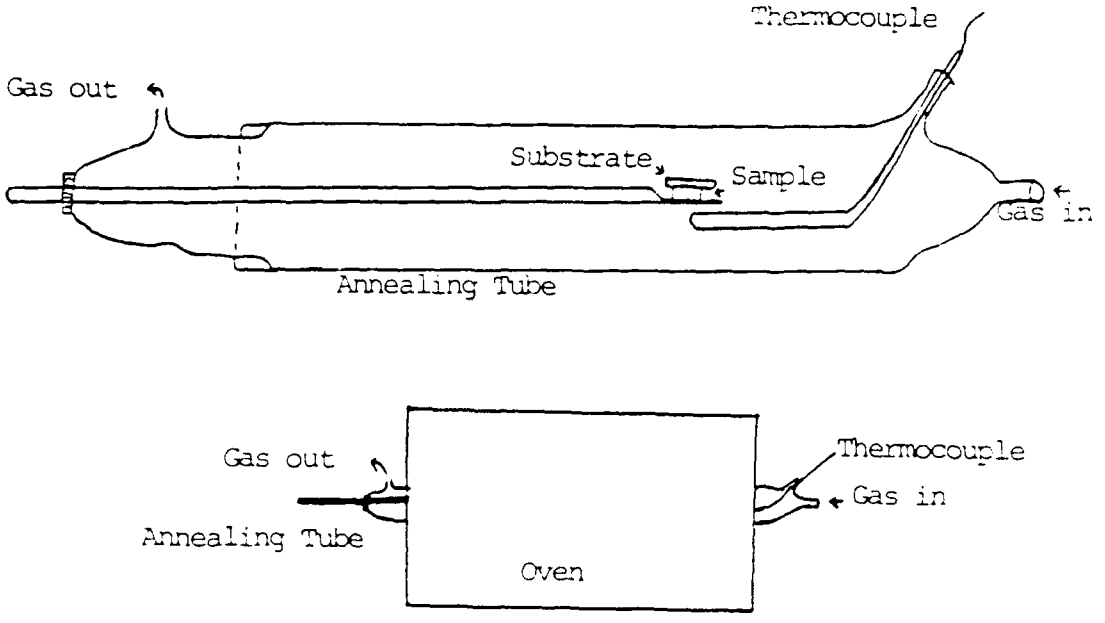

Figure 2. Conventional Furnace Annealing

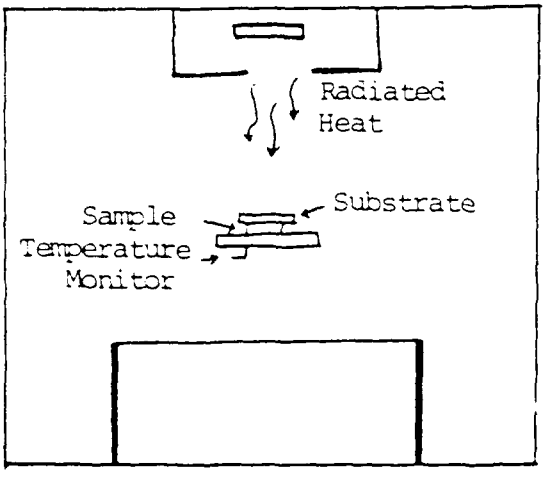

Figure 3. Rapid Thermal Annealing

wavelength associated with the specific type of transition. Although nonradiative transitions also occur, they are normally associated with lattice vibrations rather than photon emissions and cannot be studied using standard PL techniques. Some of the radiative transitions found in extrinsic semiconductors are illustrated in Figure 4 and will be discussed in the following paragraphs. Symbols for the various transitions that are commonly used by spectroscopists will be used here also (i.e. see 8:301).

Band to band recombination occurs when an electron in the conduction band recombines with a hole in the valence band. The emitted photon has an energy equal to the bandgap energy, E_g.

When a free exciton (X) recombines, it emits a photon of energy (9:114)

$$h\nu = E_g - E_x \tag{5}$$

where ν is the frequency, h is Planck's constant, and the other variables are as previously defined. When the electron and hole of a bound exciton recombine, a photon of energy (9:120)

$$h\nu = E_g - E_x - E_b \tag{6}$$

is emitted. Again, E_b is the additional energy associated with the impurity to which the exciton is bound and is typically on the order of 1 meV (8:87).

A free to bound transition occurs when either an electron from the conduction band combines with a hole in

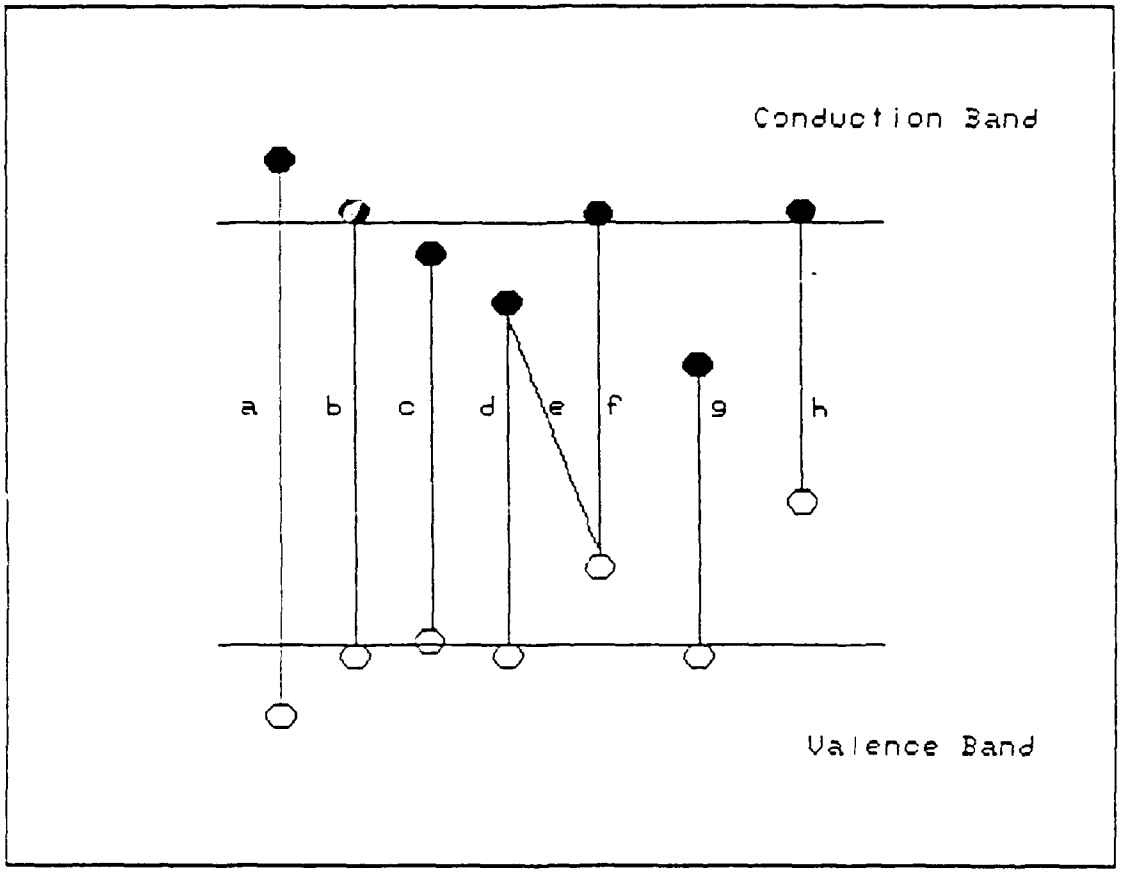

Figure 4. Electron-Hole Radiative Recombination Processes Across the Bandgap. (8:87,301)

a--Creation of electron-hole pair by optical pumping
b--Band to band recombination
c--Free exciton decay (X) (Bound exciton not shown.)
d--Neutral donor to free hole (D,h)
e--Donor to Acceptor (D,A)
f--Free electron to neutral acceptor (e,A)
g--Deep donor to free hole
h--Free electron to deep acceptor

the acceptor level (e,A^0) or an electron from the donor level combines with a hole in the valence band (D^0,e). The emitted photon has energy (9:132)

(7) $$h\nu = E_g - E_{a,d}$$

where $E_{a,d}$ is acceptor and donor ionization energy, respectively.

Lastly, donor-acceptor recombination (D^0,A^0) can occur if donors and acceptors are present at the same time in the semiconductor. Simultaneous presence can reduce the normal ionization energy due to Coulombic interaction. Therefore, a photon emitted by a (D^0,A^0) transition has energy (9:143)

(8) $$h\nu = E_g - E_a - E_d + (e^2/Kr)$$

where K is the dielectric constant and r is the donor-acceptor separation.

Selective Excitation Luminescence (SEL).

Whereas PL measurements take place with excitation energies above the bandgap, SEL takes advantage of tunable lasers to excite the sample with energies at and below bandgap. By selectively exciting specific energy regions, one can attempt to evaluate the mechanisms responsible for the transition of energy from the incident photons to the emission of lower energy photons associated with the impurities. A more thorough discussion of these transfer mechanisms will be saved for a later section.

Photoluminescence Excitation.

Photoluminescence excitation spectroscopy is another

common method used to evaluate energy transfer mechanisms. In this method a specific emission line is monitored on the spectrometer and the tunable laser is used to scan over the selected energy range at a given rate. This method allows one to determine which excitation energies cause the line of interest to increase or decrease thus allowing a study of the excitation transfer mechanism.

Phonon Replicas.

Quantum mechanically, the full ion and lattice system is given by the Hamiltonian

$$H = H_{fi} + V_c^0 + V_c^v + H_L \tag{9}$$

where H_{fi} is the free ion Hamiltonian of the dopant ion, H_L is the Hamiltonian describing the lattice, V_c^0 is the static crystal field-ion interaction energy that applies when all the ions are in their average positions, and V_c^v is the dynamic term, which is the interaction energy of the dopant ions in the time-varying crystal field (8:43).

If the interaction energy of the ion-lattice Hamiltonian is weak as it is in RE's, the calculations reveal that there is a nonzero probability of crystal field modulated FM sidebands occurring in the absorption and emission spectra. These sidebands are displaced by an integral number of phonons to the high energy side in absorption and to the low energy side in luminescence (8:47). The sidebands are also called phonon replicas; they play a key role in the spectrum of InP:Yb. The transverse

optical phonon (TO) displacement has been found to be approximately 38 meV for this material (12).

Properties of Rare Earth Elements in Semiconductors

The rare earth elements, or lanthanides, are those elements of the periodic table that have atomic number between 58 and 71 inclusive, beginning with cerium and ending with lutetium. They have similar chemical and physical properties that make them quite interesting and appropriate for many applications.

The luminescence of semiconductors doped with rare earths have been found to contain sharp emissions characteristic of the particular rare earth and host crystal. It has been determined that the variety of luminescence lines is attributed to the intra-4f transitions and to the formation of complexes between lanthanides, defects and host atoms. In general, the RE related luminescent structure of RE doped semiconductors is very complex; in these cases the symmetry of the RE related centers is believed to be low (13). The emission lines are due to internal electronic transitions of the 4f electrons of the triply ionized lanthanide. In the simplest and most thoroughly analyzed RE doped semiconductor, InP:Yb, the very sharp and intense emissions near 1 μm are characteristic of the transitions between spin orbit levels of Yb^{3+}, $^2F_{5/2}$ and $^2F_{7/2}$ (14). The spin orbit levels are then further split by the crystal field.

The electronic configuration of the rare earth element can be written as

$$[Xe]4f^n5d^m6s^2$$

where $n = 0..14$ but $n \neq 2,8$, and $m = 0,1$. In particular, the electronic configuration for Yb can be written

$$[Xe]4f^{14}6s^2$$

and for Yb^{3+} the full electronic configuration is

$$1s^2 2s^2 2p^6 3s^2 3p^6 3d^{10} 4s^2 4p^6 4d^{10} \underline{4f}^{13} 5s^2 5p^6$$

where the underline is added to emphasize the unfilled subshell. The transitions of interest are 4f-4f and there are full subshells outside the shell responsible. The outer shells shield the inner shells from the crystal field to a degree and are responsible for the sharpness of the characteristic RE emissions. They also restrict the crystal field's effect on the spin orbit level splitting so that the overall effect on the spectra is relatively small.

In an equation similar to equation (9), the Hamiltonian for a RE ion incorporated into a crystal lattice can be given by

$$H = H_{fi} + H_L + V \tag{10}$$

where V is the very small ion-lattice coupling and the symbols are the same as in equation (9). Since V is usually small the total Hamiltonian can be treated as the sum of the solutions of two uncoupled Hamiltonians that can be solved separately. V can then be treated as a perturbation to the system. Solutions very close to the free ion solutions are

the result of this line of treatment.

Previous Research

Considerable research has been accomplished over recent years in the study of RE doped III-V semiconductors. This section will briefly outline the significant experiments and findings as related to the current work.

Although there was a brief effort to examine the luminescence of RE doped III-V semiconductors in 1964 with intermittent interest thereafter, it was not until the 1979-1980 time frame that substantial efforts were reported. In 1980, Kasatkin reported the first 4f-4f transitions in GaP:Yb and in 1981 Zakharenkov reported the photo-luminescence of InP:Yb (4,5). Significant research efforts were then undertaken in the Federal Republic of Germany, the United States, Poland, and Japan. Experimental and theoretical results have led to the formulation of an energy level structure for InP:Yb, the most widely studied RE doped semiconductor. Efforts in recent years have also led to the development of an InP:Yb LED and an InGaAsP:Er laser (2,3).

Ennen et al used high resolution spectroscopy to resolve 17 sharp luminescent transitions of Yb implanted InP in 1984 (16). His line number convention is illustrated in Figure 5 on a spectral plot taken during this current research effort; all future reference to specific line numbers will correspond to the convention established by

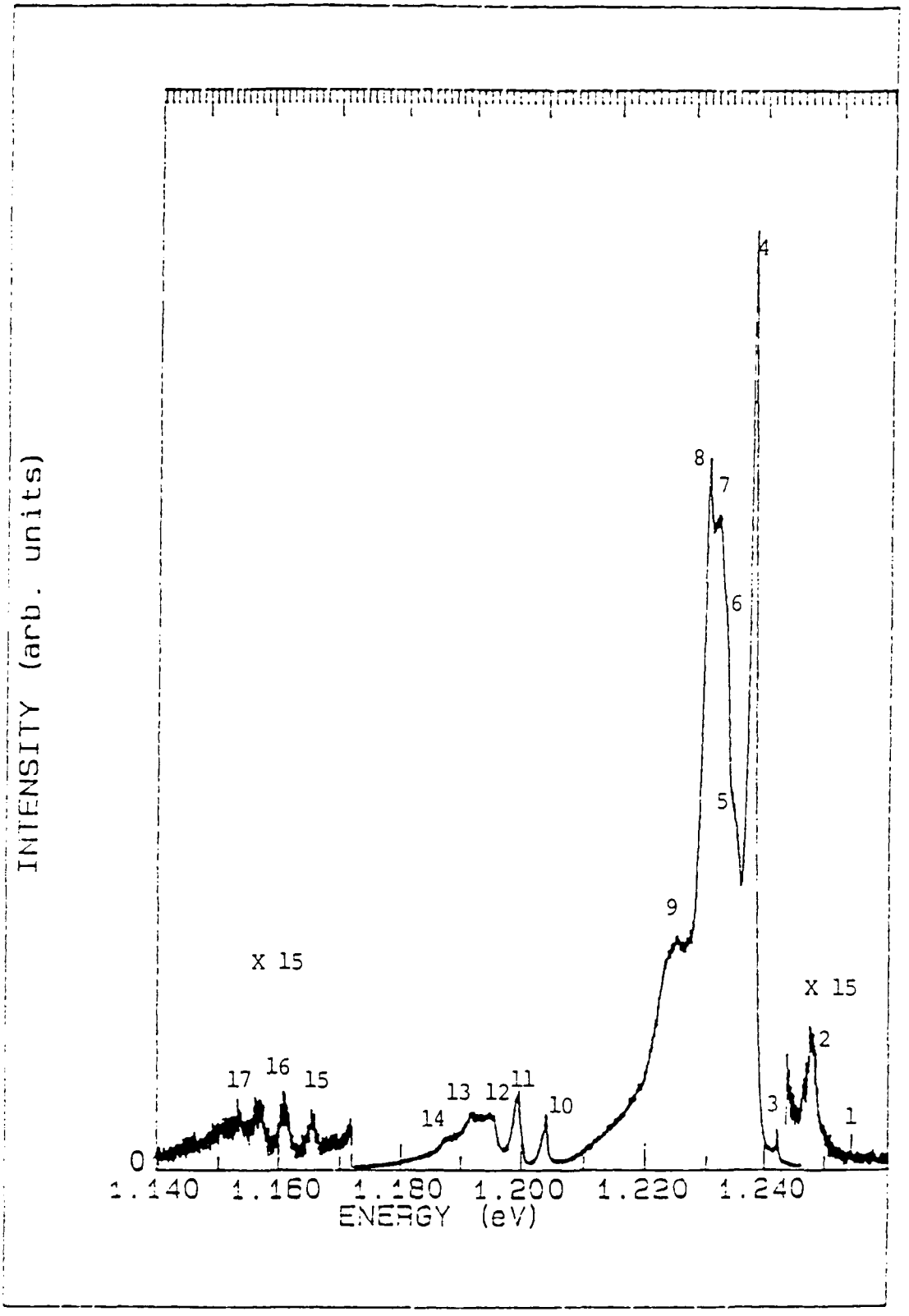

Figure 5. Line Identification of Yb Related Emissions of InP:Yb as Defined by Ennen et al. (16,18)

Ennen et al as shown in this figure.

Zeeman analysis by Aszodi et al showed that the overwhelming part of the Yb induced emission in InP arises from only one type of luminescent center on a cubic site, and that triply ionized atoms lie on unperturbed indium sites with tetragonal (T_d) symmetry (1). In a potential with symmetry T_d, the J = 5/2 sextet (2J + 1 degeneracy) will split into Γ_8 and Γ_6 states and the J = 7/2 octet will split into Γ_8, Γ_7 and Γ_6 (1). The irreducible representations of T_d are the notation of Koster et al (17). The energy level diagram shown in Figure 6 is consistent with the Zeeman data and with PLE measurements taken by Ennen (16). Lines 2, 3, 4 and 8 of Figure 5 are evidently the zero-phonon transitions from the upper spin orbit level $^2F_{5/2}$ to the ground spin orbit level $^2F_{7/2}$. Lines 10, 11, 12, 13, and 14 are one-phonon replicas and lines 15, 16 and 17 are two-phonon replicas. Only line 1, which is a weak but extremely sharp emission is attributed to a noncubic symmetry; it was found to arise from a trigonal Yb-X defect complex (18). Line 2 was further identified as a "hot line" corresponding to line 3. The "hot lines" corresponding to lines 4 and 8 occur at 996.5 and 1002.7 nm, respectively, but because of line broadening at higher temperatures, these lines were not seen.

Although the above assertions are generally well accepted, cluster calculations done by Hemstreet in 1986

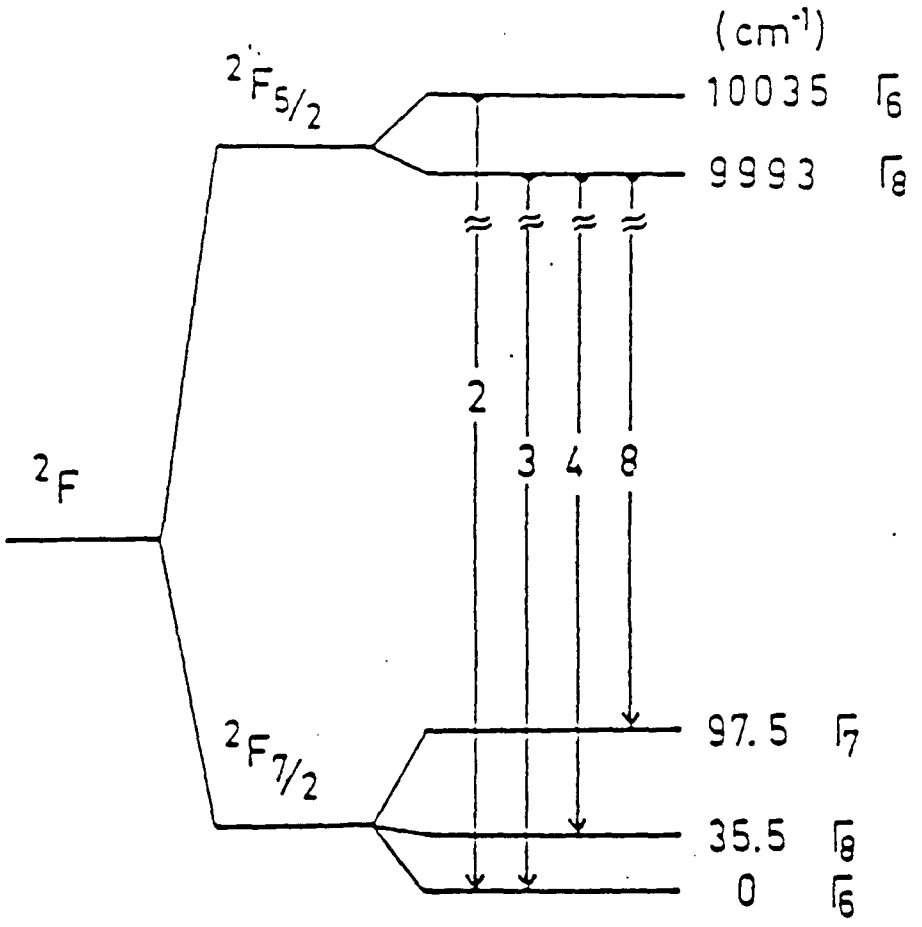

Figure 6. InP:Yb Energy Level Diagram

predict the energy level scheme shown in Figure 7. (Although different, Hemstreet recognizes the difference between the two diagrams is minimal and well within the error of his measurements.) His calculations suggest that the stable ground state of a neutral substitutional Yb impurity in InP is neither $Yb^{2+}(f^{14})$ (proposed by some as necessary for bonding (19)) nor $Yb^{3+}(f^{13})$ but corresponds to a configuration intermediate to the two. According to the calculations, there is one hole in the impurity manifold in the gap and Yb should behave as a single acceptor with a hole ionization energy of approximately 0.26 eV. Hemstreet also claims that the atomic-like Yb^{3+} ion that is observed in the luminescence experiments is not a stable charge state of the cluster and appears only upon excitation of a hole in the $j = 5/2$ component of the impurity f states (20). Klein supports Hemstreet's findings and proposes that the coexistence of the neutral acceptor state, Yb^{2+}, and the internal Yb^{3+} core state is not necessarily inconsistent (19).

Research on the luminescence properties of Yb doped GaAs was initiated more recently than InP:Yb. Although Ennen et al reported a characteristic Yb emission (16,18), other researchers (13,21) have shown that Yb luminescence from GaAs is unlikely and were unable to achieve it. Raczynska et al proposed that the presence of Yb during growth of LPE GaAs:Yb layers caused strong suppression of

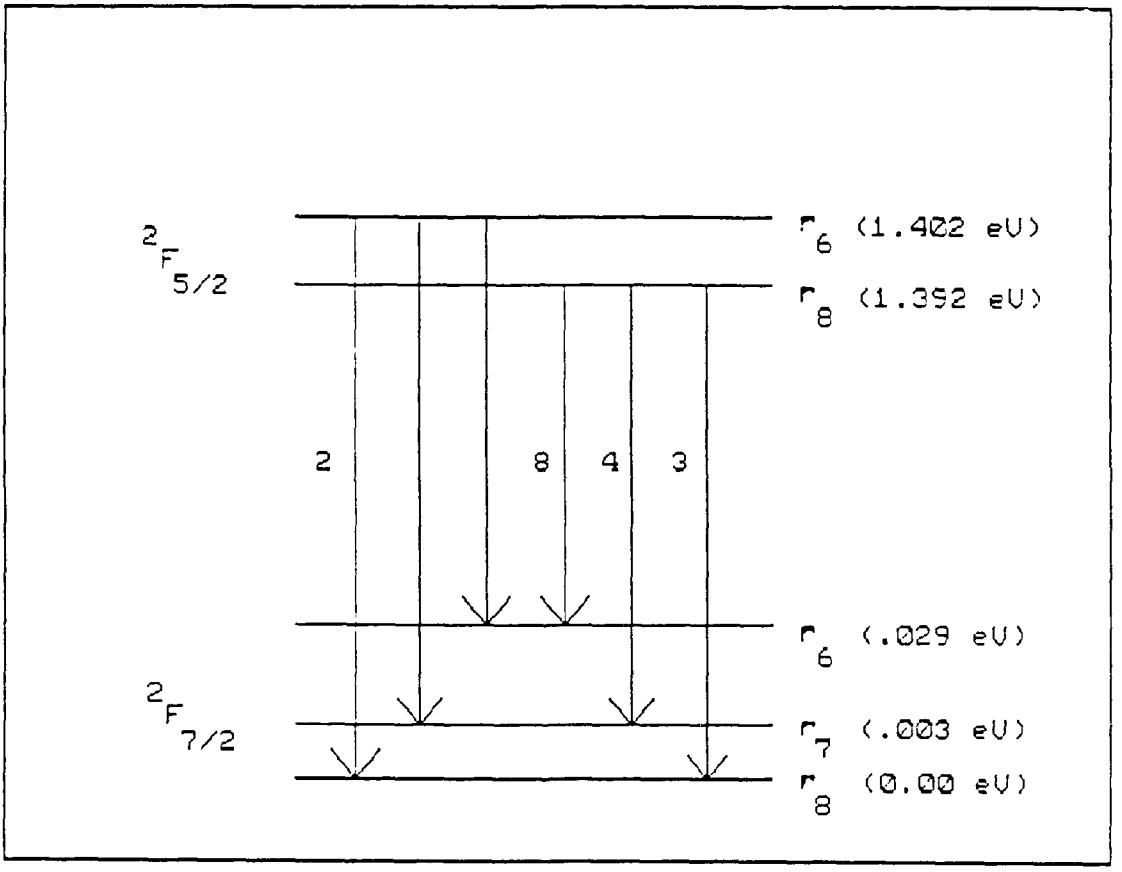

Figure 7. InP:Yb Energy Level Diagram as Derived from Cluster Calculations. (20)

all donor related optical transitions due to the effective removal of donors (21). This, then, prevented Yb emission.

Kozanecki and Gröetzschel emphasized that the T_d symmetry shown in InP:Yb was established only for that material (13). Their investigations demonstrated that implanted Yb diffused to the surface and formed precipitates in GaAs. In addition, they showed through the use of Rutherford backscattering that only a small fraction of the implanted ions occupied substitutional sites. For these reasons there was no Yb emissions from their samples. Nakagome et al conducted secondary ion mass spectrometry (SIMS) measurements on LPE InP:Yb and other doped III-V semiconductors and found that the RE ions were, indeed, not uniformly dispersed but were incorporated as "micro-particles of rare-earth-ion-rich compounds." (22)

Gippius et al directed their a ention specifically at the effect of defects on RE implanted material (23). They found that as a general rule, the number of lines observed in PL measurements corresponding to a certain pair of spin orbit terms far exceeded the number of allowed transitions for cubic centers. They concluded that the majority of the lines were due to complex centers of lower symmetry.

The first case of Yb implantation into AlGaAs was reported by Colon in 1988 (24). The signals were weak and were not located at the same wavelength for each of the three aluminum molar concentrations evaluated (x = .15, .23,

and .30), indicating significant effect on the luminescent center by the Al atoms in the lattice or that the defects had the dominant influence on the luminescence.

Excitation and Decay Mechanisms

In the mid- 1980's, InP:Yb research efforts largely transitioned from the investigation of the structure of the RE related centers to the excitation and decay mechanisms of these luminescent centers. Wagner et al in 1984 demonstrated direct Yb luminescence by exciting the sample at 993 nm (wavelength of line 2). Lines 4, 7, and 8 appear just as they did for below bandgap and the one phonon displacements also appeared (25). Their spectra appears in Figure 8.

Using photoluminescence and electroluminescence on InP:Yb, Kasatkin et al proposed that shallow donor-acceptor impurities play the dominant role in the photoexcitation of intracenter luminescence of InP:Yb and GaP:Yb (26,27). While exciting in the range of 1.395 to 1.420 eV the excitation of the donor-acceptor pair luminescence had a dip where there was a sharp maximum in the Yb^{3+} luminescence; in the undoped InP, there was no dip. When they increased the Yb concentration to $10^{17}/cm^3$ the Yb quenched the donor-acceptor luminescence and Yb signal duplicated the no-Yb sample. Figure 9 shows their results graphically (26).

A third excitation mechanism was promoted by Körber and Hangleiter. They conducted other experiments using PLE that

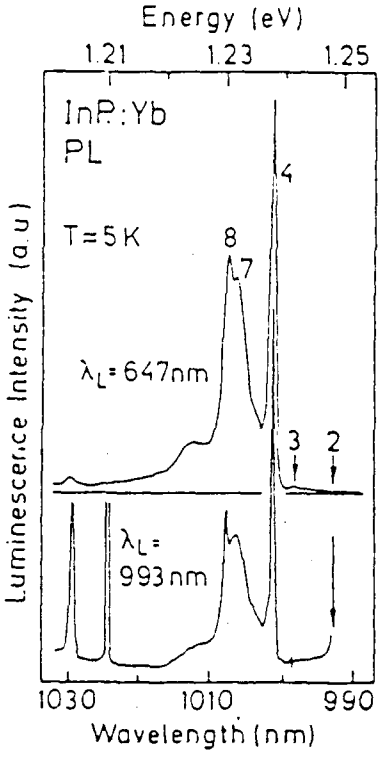

Figure 8. Spectra of InP:Yb with Excitation at 647 nm (upper trace) and 993 nm--Resonance with Line 2 (lower trace). (25)

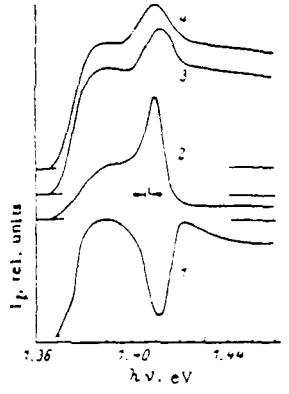

Figure 9. Excitation Spectra of the Donor-Acceptor Pairs (1) and Yb (2) Luminescence Exhibited by InP:Yb when Concentration of Donors/Acceptors is Much Greater than Concentration of Yb. Spectra of Pairs in Undoped InP (3) and of Yb in InP:Yb when Yb Concentration is Greater (4). (26)

contradicted Kasatkin's findings and instead proposed that free carriers are required to excite the Yb centers. They suggested that the actual excitation may occur by direct capture of excitons or by impact excitation by hot carriers that could be generated by Auger processes (28).

Using time resolved photoluminescence, Körber and Hangleiter found the lifetime of the excited state of Yb to be 12.7 ± 0.4 μs regardless of doping method, Yb concentration, or line chosen for study (which further adds credence to the theory that all Yb lines originate at one luminescent center) (28). However, Yb^{3+} $^2F_{5/2}$ lifetimes in ionic crystals have been found to be much longer (≈ 1-3 ms); the large difference must be due to nonradiative processes. Since Yb in InP acts as a shallow acceptor, they proposed that the Yb decay may be similar to the Auger decay of acceptor bound excitons. Here the energy of the excited state is transferred to the bound hole, which is deeply excited into the valence band (22). Figure 10 illustrates this decay process. In a separate analysis, Klein reached the same conclusions as Körber and Hangleiter (19).

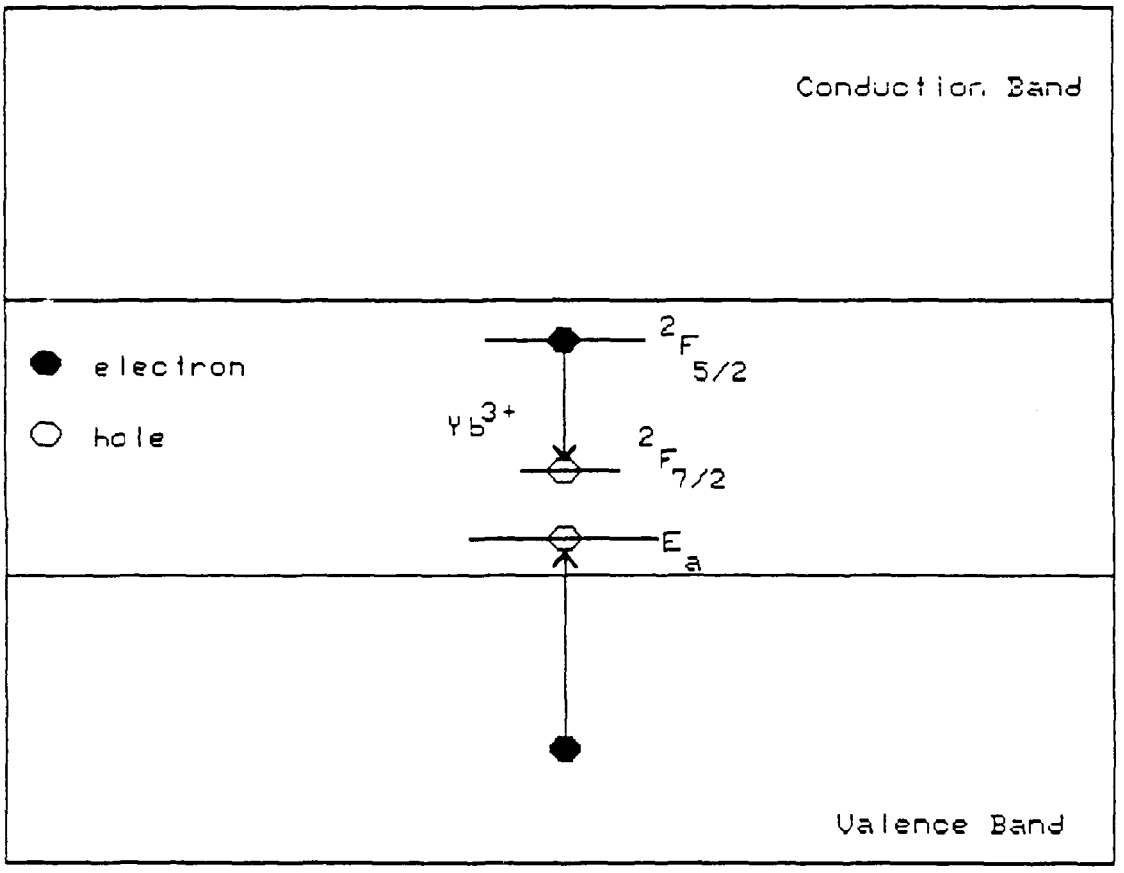

Figure 10. Decay Process of Yb Related Emissions in InP:Yb as Proposed by Korber and Hangleiter. (28)

Experiment

The equipment used in this research was for the most part previously configured in a manner suitable for this investigation and had been used for both PL and SEL experiments in the past. The general system consists of four main parts:

1. Excitation System
2. Cryogenics System
3. Optical Detection System
4. Data Acquisition System.

The following sections contain detailed information about these systems and general comments about system integration. Figure 11 illustrates a typical experimental setup and schematics for each system are contained in subsequent figures. The last section describes sample preparation procedures followed for each sample prior to an investigation of its luminescence.

Excitation System

Argon Ion Laser.

The excitation source used for all PL investigation and for pumping the dye laser for SEL measurements was a Spectra Physics (SP) Model 171-19 argon ion laser. It was initially capable of pumping with seven watts in the "all-lines" configuration. A new plasma tube was installed late in the research period that allowed optical pumping of almost 20 watts. This greater power allowed a somewhat higher

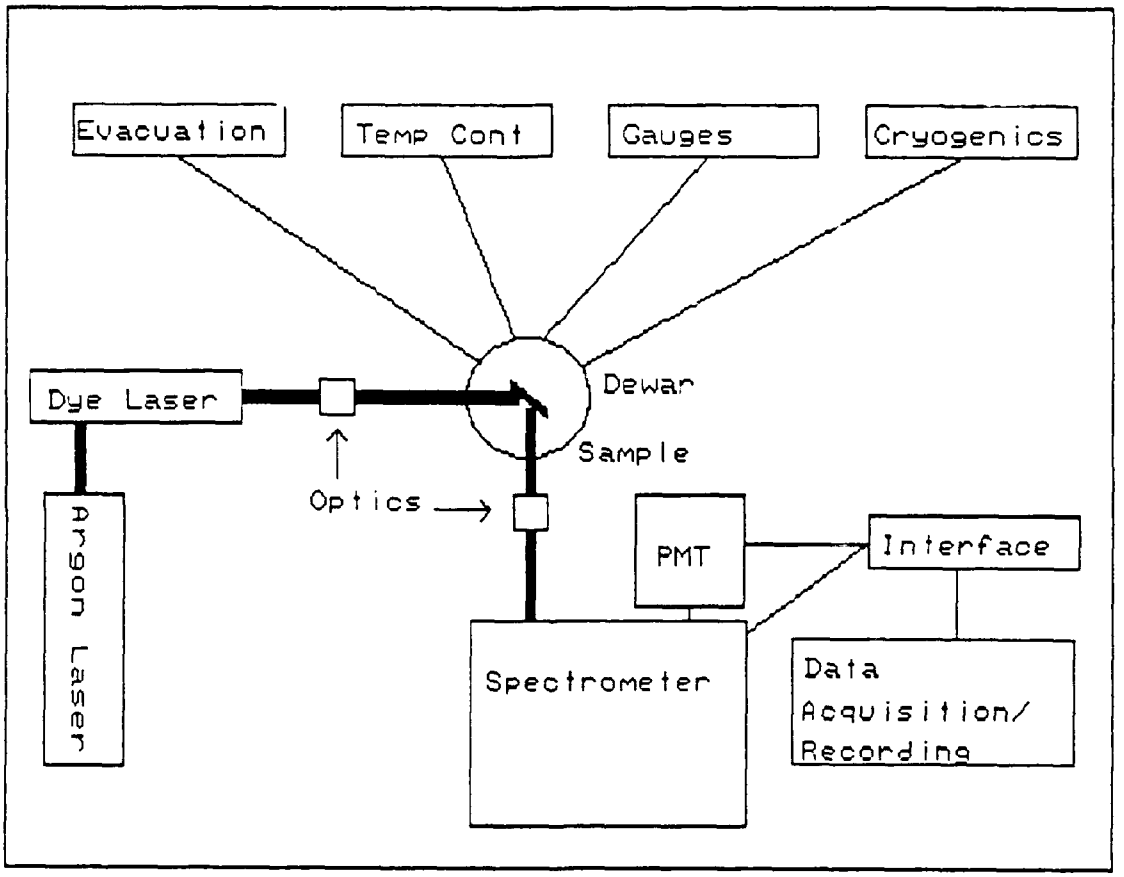

Figure 11. Experimental Setup

wavelength to be used for the SEL measurements but dramatically reduced dye lifetime. Although the laser transitions occurred at many wavelengths in the "all lines" mode, the strongest transitions occurred at 488.0 nm and 514.5 nm. These were the principle lines used for PL measurements since a narrow band interference filter centered at 495 nm was placed in the beam path.

Tunable Dye Laser.

The dye laser used for all SEL measurements was a SP Model 375-50 with a continuous flow, variable pressure supply and filtering system. The dye laser is capable of adjustable lasing in small bands over a wide range of wavelengths from ultraviolet to infrared. The bands available at any one time depend on the mirrors installed and the type of dye used in the system. The dye that allows the highest wavelength excitation is Exciton's LDS 821 that is advertised to lase over a band from 830 nm to 965 nm with a peak power of 360 mW (with extended range mirrors installed). In practice, however, the laser put out a maximum peak of 280 mW and a power output of only 10 mW at 900 nm. The major drawback to this laser system is that the dye does not maintain its maximum capability for more than a few hours of use; therefore, investigations above approximately 870 nm were rare and above 900 nm nearly impossible.

The tuning of the laser inside the chosen band was

accomplished by manually turning (with a micrometer) a triple plate birefringent filter located within the laser cavity.

Figure 12 illustrates the excitation sources. Although the figure shows the argon ion laser in its dye laser pumping mode, a mirror placed between the two lasers can be used to redirect the beam for PL applications.

Cryogenics System

The cryogenics system consisted of a Janis vacuum dewar with a detachable tail, a mechanical oil pump and diffusion pump for evacuating the dewar's vacuum chamber, another mechanical pump to evacuate the sample chamber, and a DRC 82C temperature controller. To conduct the experiment, the samples were placed on a cold finger that was inserted into the dewar from the top. With liquid helium in the helium chamber the temperature of the cold finger could be lowered to 4.2K by allowing helium to flow into the sample chamber through a needle valve and capillary tube. By evacuating the sample chamber as helium is flowing, the temperature could be further lowered to 2.5K--a procedure known as lambda pumping.

A mechanical pump was used as a rough pump to reduce the vacuum pressure from atmospheric to approximately 30 microns. With the diffusion pump, the pressure was further reduced to 0.5 microns.

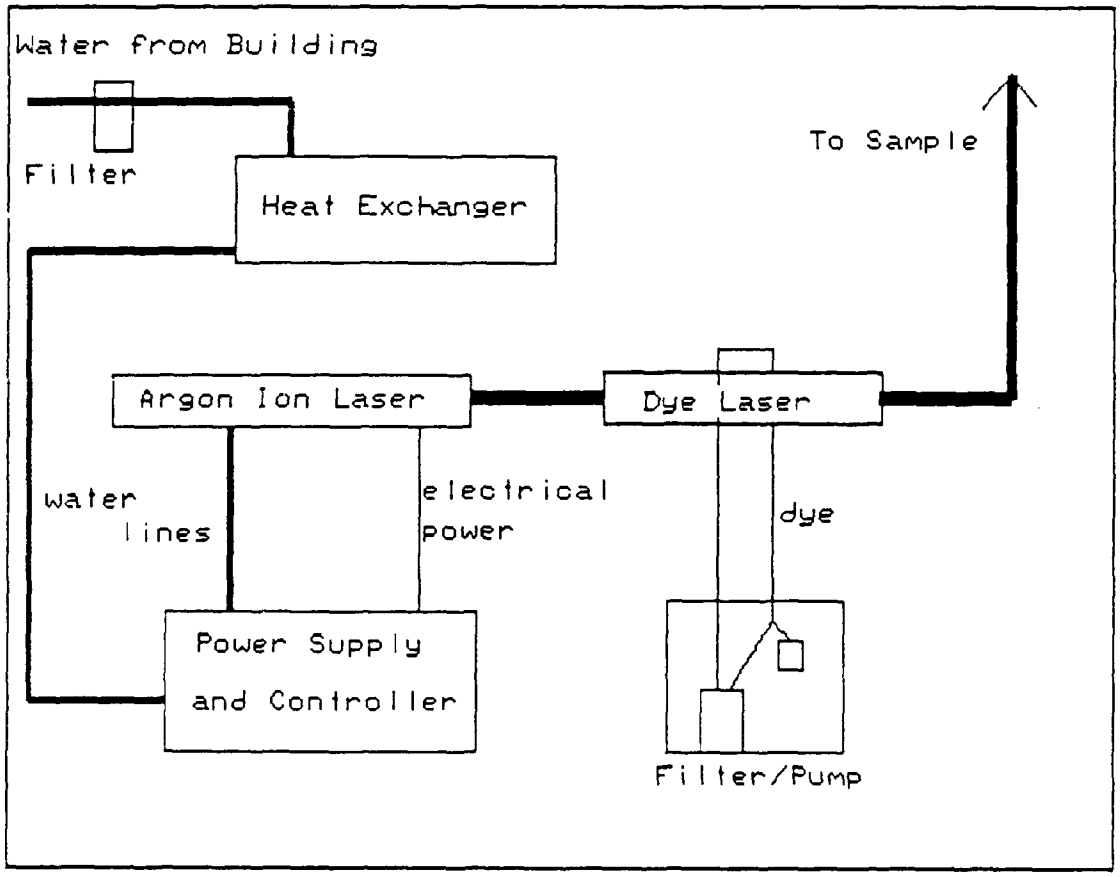

Figure 12. Excitation System

The sample chamber pressure could be evacuated with a separate mechanical pump that was capable of reducing the pressure to approximately 8 torr. Two modifications were made to the system during this research: 1) a vacuum valve was added in the line between the mechanical pump and the dewar to allow control of the sample chamber pressure, and 2) an additional line with a vacuum valve was installed from the mechanical pump to the helium reservoir to allow evacuation of the helium chamber. The goal of the second modification was to prevent the commonplace freeze-ups of the needle valve and capillary tube by removing any water vapor, nitrogen gas, or air that entered into the system.

Figure 13 illustrates the cryogenic system. The sketch of the dewar represents a top view where the circles depict the sample chamber, the helium reservoir, and the outer vacuum wall.

Optical Detection System

The heart of the optical detection system was the Spex 1702 3/4 meter Czerny-Turner spectrometer with a 1200 lines/mm grating blazed at 5000 Å. The resolving power of the grating in the first order was 1.16×10^5 which allowed maximum resolution of approximately 0.1 Å wavelength difference at 1 μm. However, the spectrometer's overall resolution is also dependent upon the slit sizes and many other factors.

Many of the experiments were conducted with the

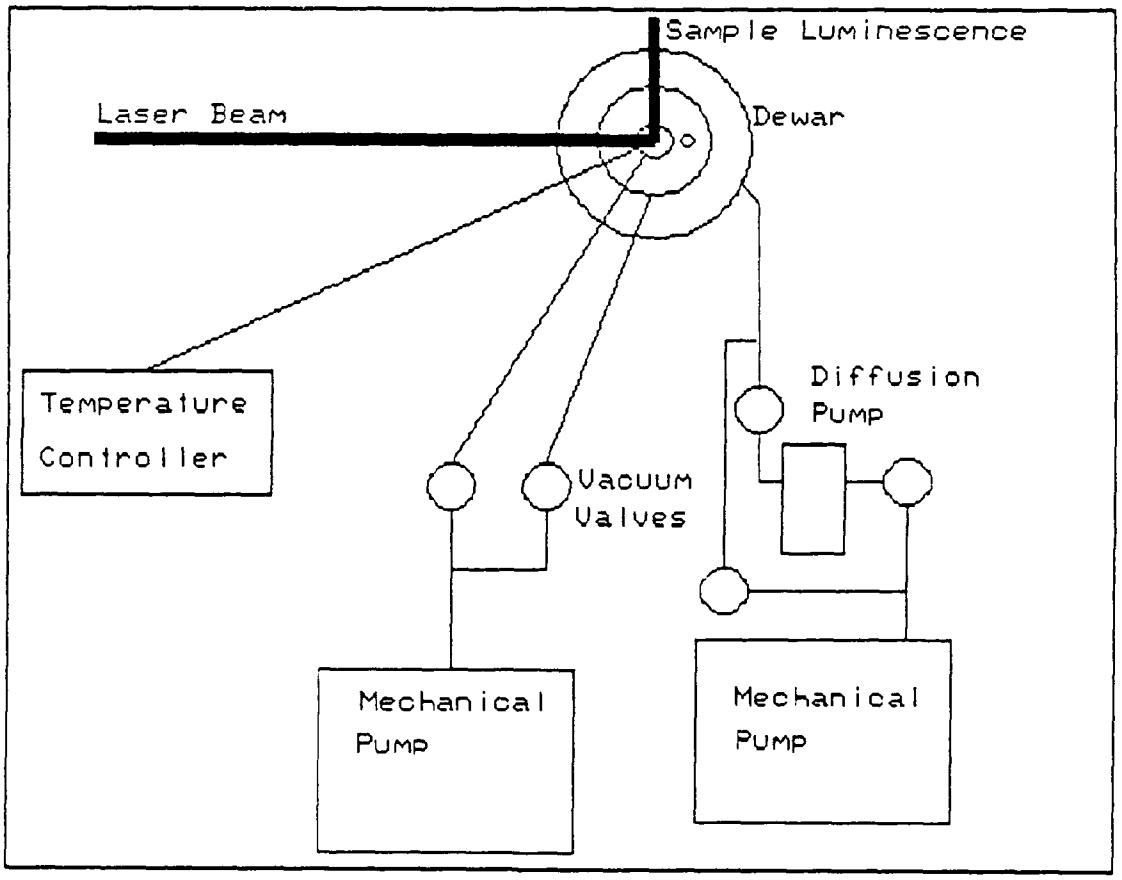

Figure 13. Cryogenics System

entrance slit at 1.5 mm and exit slit at 3.0 mm for low resolution but high intensity since the lines of interest were weak and well separated. Other parts of the experiment were conducted with the entrance slit at 75 μm or 100 μm and exit slit at 150 μm or 200 μm, respectively, for high resolution. In all cases, the exit slit was set at twice the entrance slit as recommended by the manufacturer.

A liquid nitrogen cooled photomultiplier tube (PMT) with S-1 responsivity was used to detect the spectrometer output. -1500 volts were applied to the PMT and it was cooled to approximately -90°C. This combination allowed for the optimum signal to noise ratio. Due to the relatively small wavelength region examined with the S-1 PMT, no correction for the system's spectral response was made.

The output of the PMT was fed into either a picoammeter or a Princeton Applied Research (PAR) model 1121A amplifier/discriminator which fed into a PAR model 1112 photon counter and into the data acquisition system. The picoammeter proved to be particularly useful for finding a particular wavelength on the dye laser. By setting the spectrometer to the selected wavelength, say 870 nm, the dye laser's birefringent filter could be turned until a response was indicated on the ammeter. At even the smallest slit sizes this technique requires OD 4 or OD 3 neutral density filters prior to the entrance slit to prevent saturation of the PMT. When the PMT was connected to the amplifier/

discriminator/photon counter, the spectral response could be recorded through the data acquisition system while being monitored visually on the photon counter. Figure 14 illustrates both the optical detection and data acquisition systems.

Data Acquisition System

From the discriminator/amplifier, the spectral data is fed into a Tracor Northern model TN-1710A multichannel analyzer (MCA) through an interface box. The MCA presents intensity of the signal as a function of individual channels. The interface box allows selection of the MCA's internal scan rate and also the spectrometer's scan speed through its external trigger mode. An argon calibration lamp was used to calibrate the spectrum and to initially compute angstroms per channel presented on the MCA scope.

Once the spectra was stored on the MCA it was transferred to a Zenith Z-100 personal computer and stored on floppy disks.

System Integration

On many of the initial spectral plots, there were many unexplained signals. In most cases these were eliminated by appropriate placement of optical filters in the path of the laser beam or the sample's luminescence. The following paragraphs outline the attempts made in this research to eliminate unwanted spectral lines.

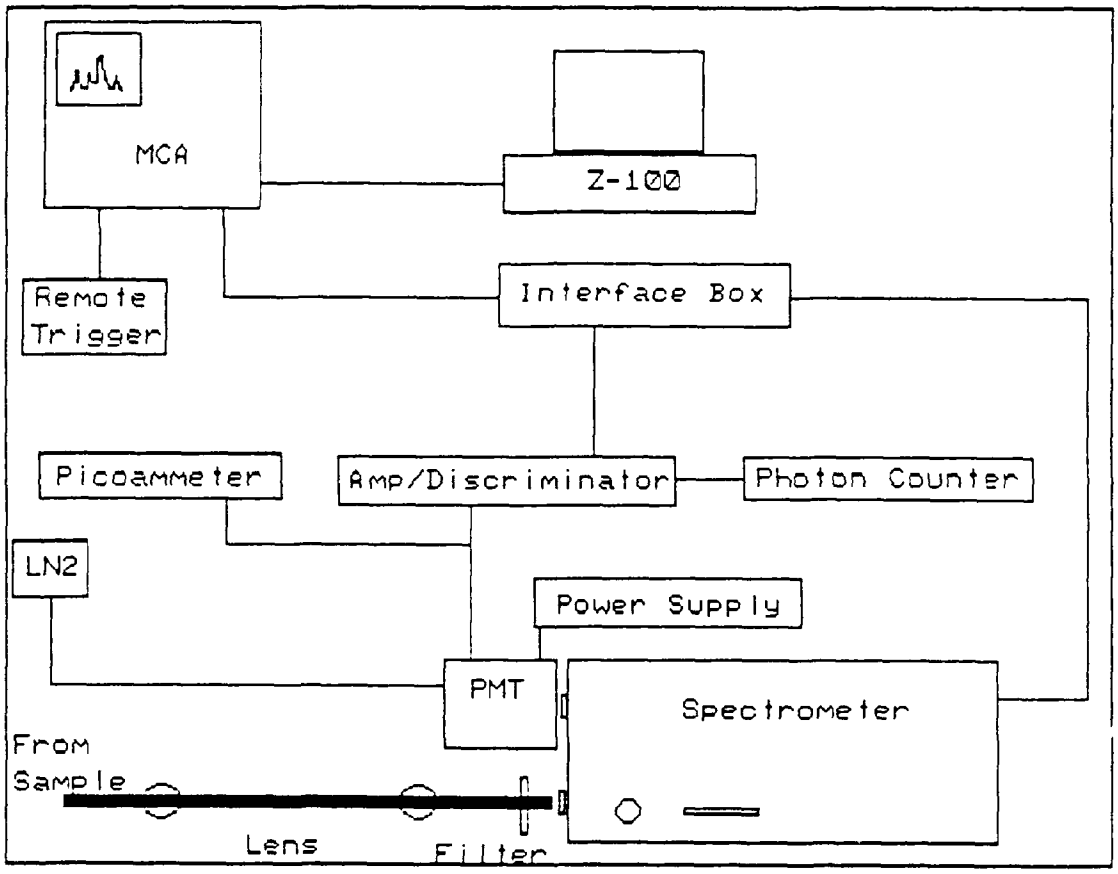

Figure 14. Optical Detection and Data Acquisition Systems

As mentioned earlier, the argon ion laser has lasing transitions over a wide range. When it was used for PL, many of the transition wavelengths were detected by the PMT. This problem was significantly reduced by placing a narrow band interference filter with peak transmission at 495 nm in the laser beam prior to its illuminating the sample. Thus, only the strongest laser lines, 488.0 nm and 514.5 nm, were able to reach the target.

Without a filter prior to the entrance slit of the spectrometer, the spectral plot often included various second order lines from the laser, sample or calibration lamp. These signals were effectively eliminated by placing a LP 695 long pass filter at the entrance slit.

A 10 cm focal length lens was used to focus the laser beam onto the sample. This allowed adjustment of the irradiance of the beam by moving the lens forward or backward to change the beam size on the sample without changing the total power. Various irradiances were used for this study--from 90 mW/cm^2 to as high as 5.3 W/cm^2.

Since the spectrometer was located about 107 cm from the tail of the dewar, a method was devised to collect the maximum amount of light. This method required one 13 cm focal length lens placed one focal length away from the sample and another of the same focal length placed the same distance from the spectrometer's entrance slit. The first lens collected light over a large solid angle and converted

the beam to parallel rays. The second lens focused the parallel rays onto the entrance slit. The lens were carefully chosen to ensure the second lens f/# closely matched the spectrometer's f/#, a condition that aids in achieving the maximum resolving power from the spectrometer.

Sample Preparation

As mentioned earlier, each sample investigated had previously been examined in various experimental setups. Some of the samples were scratched, marred or chipped but most were just smudged or had glue residue on them. Regardless of their condition each specimen was thoroughly cleaned with an application of trichloroethylene, acetone, and methanol. Trichloroflouromethane gas was used to dry the samples.

To hold the samples on the copper cold finger, a very slight amount of vacuum grease was placed on a back corner so as to not induce stress. Up to four samples could be mounted simultaneously, two each on opposite sides. A mask with 6 mm circular holes was then placed over each side.

Results and Analysis

In this section the experimental results of this research will be presented and analyzed. The first section will analyze the results of work done on Yb implanted bulk grown InP; the second will deal with an analysis of Yb implanted VPE InP; and the last will discuss the results of GaAS and AlGaAS photoluminescence.

Yb Implanted Bulk Grown InP

Two specific experiments were conducted on an Yb implanted InP sample that was annealed at 850°C for 15 seconds using the RTA method after being implanted at 1 MeV with 3×10^{13} *ions/cm*^{2}. It was "proximity capped" to reduce phosphor loss during annealing. The first experiment was a study of the intensity of all known Yb emissions near 1 *μm* as a function of total incident power. The argon ion laser was used as the excitation source and neutral density filters were used to step down the incident power. With a beam diameter of 2.23 mm the spectral intensities were measured at irradiances of 5.3 W/cm^2, 4.6 W/cm^2, 2.8 W/cm^2, 1.9 W/cm^2, 0.5 W/cm^2, 132 mW/cm^2, 5.3 mW/cm^2, and 0.53 mW/cm^2. A plot of the spectrum taken at 5.3 W/cm^2 was shown in Figure 5. Of particular interest is that line 1 is easily seen at the higher irradiances, indicating the presence of this particular defect.

Figure 15 illustrates the changing intensity pattern with the reduction in irradiance. As expected, as the incident power is decreased there is an associated decrease in the intensity of each Yb line. Figure 16 graphically illustrates the change in intensity for the zero phonon lines 2, 3, 4, and 8. As can be seen from the figure, as the incident power increases, lines 3, 4, and 8 begin to saturate and flatten out. Line 2, however, shows the opposite effect--that the intensity of that line increases dramatically as the incident power is increased. Two possible explanations for this exist. The first possibility is that as more and more electrons are excited out of the ground $^2F_{7/2}$ state and into the upper spin orbit $^2F_{5/2}$ excited state, they saturate the Γ_8 level causing the Γ_6 population to increase. As this level population increases more radiative transitions can occur from the Γ_6 level--a transition corresponding to line 2.

The other possibility is that the higher incident powers cause localized heating, thereby thermally activating some of the Γ_8 level electrons into the Γ_6 level of the $^2F_{5/2}$ spin orbit state. This mechanism would also result in increasing intensity for line 2 by causing it to exhibit its "hot line" characteristics.

By further examining the InP:Yb structure at high incident power one can resolve possible emission lines that have previously been unreported. Figure 17 shows line 12a

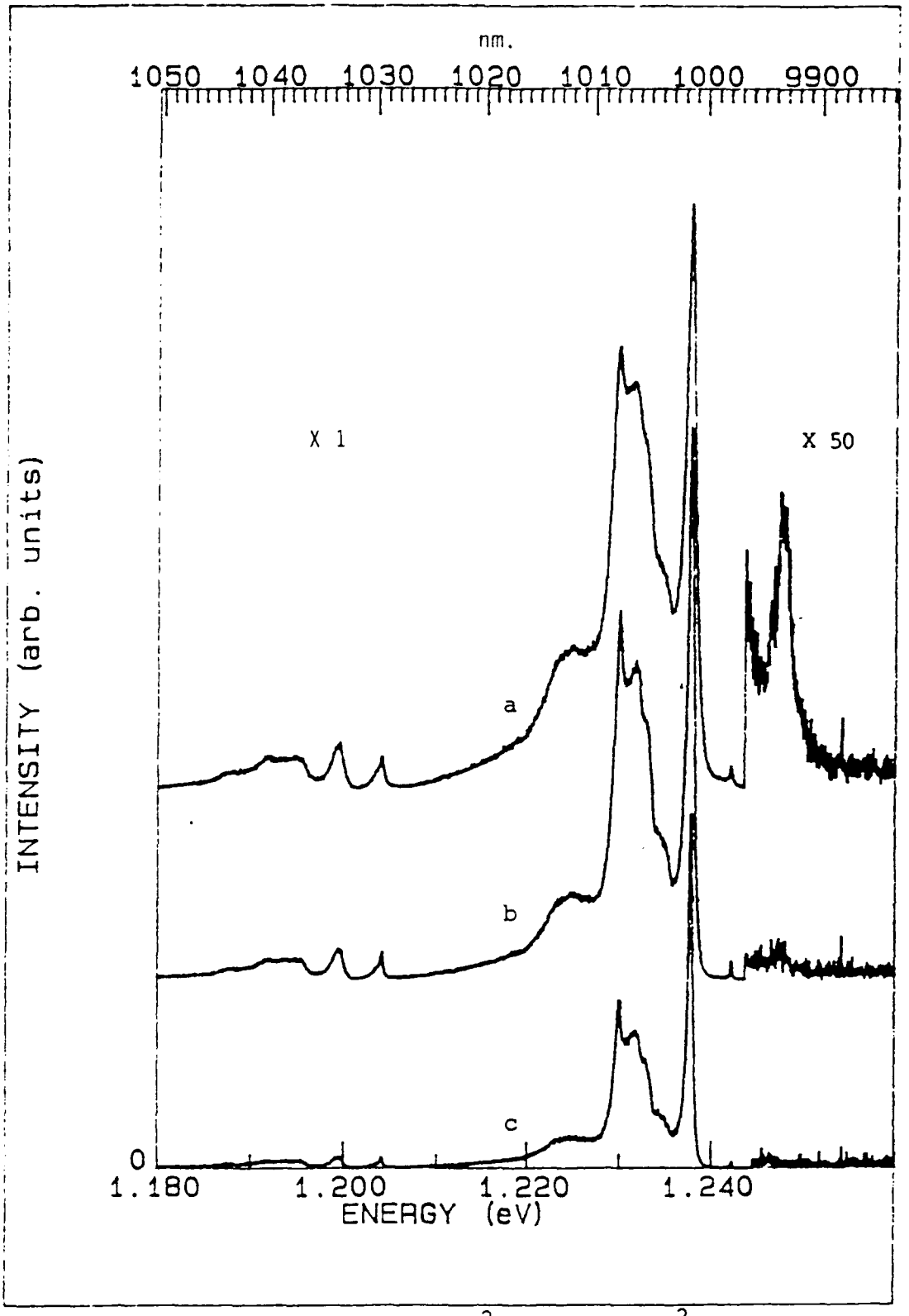

Figure 15. PL of InP:Yb at 5.4 W/cm^2 (a), 1.9 W/cm^2 (b), and 0.13 W/cm^2 (c).

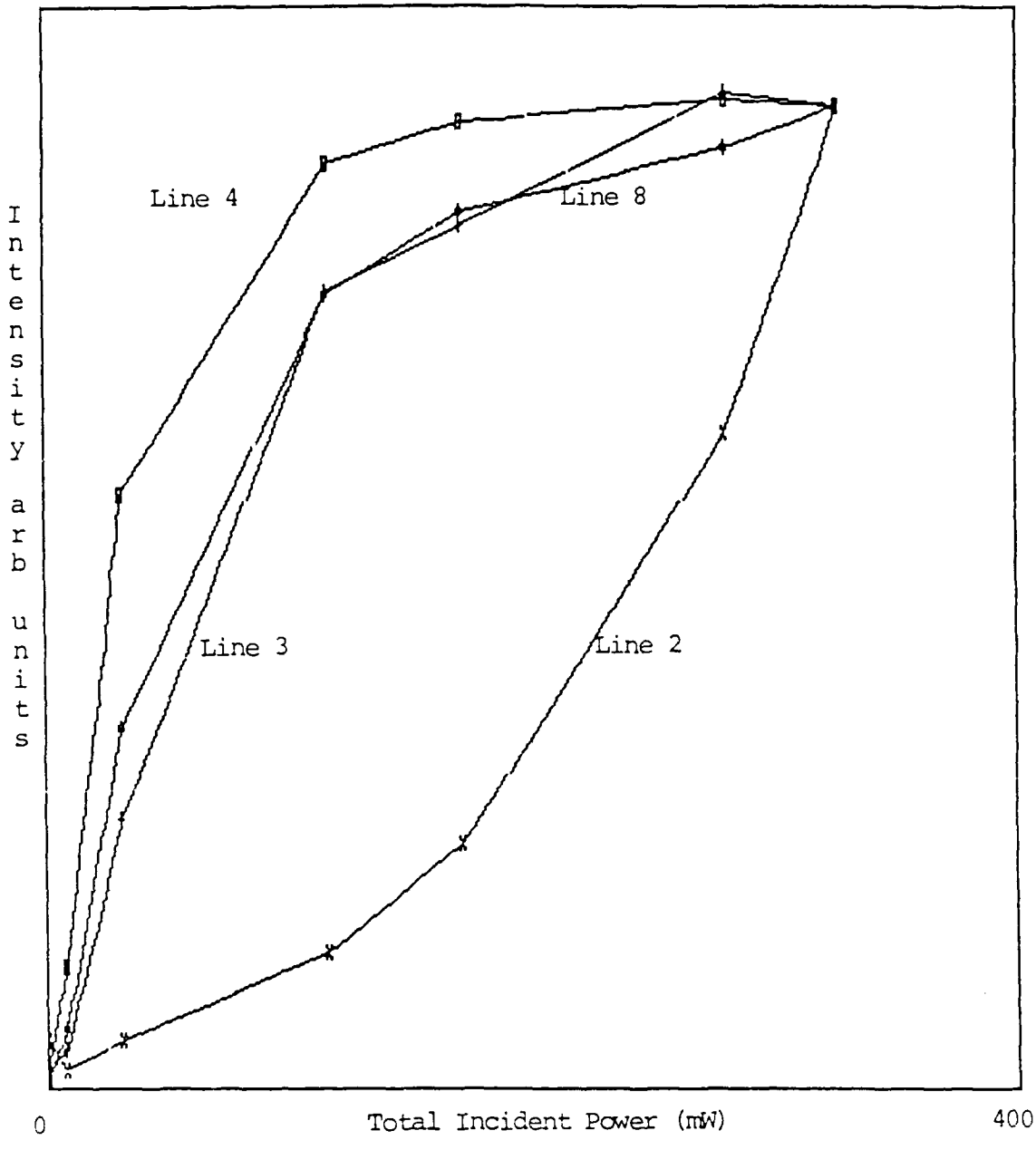

Figure 16. Intensity Changes of Lines 2, 3, 4, and 8 of InP:Yb as a Function of Total Incident Power. Intensities Normalized to One for Comparison. Sample Temperature = 7K.

at 1.1940 eV and Figure 18 shows line 17a at 1.1538 eV. Line 12a corresponds to a one transverse optical (TO) phonon displacement of line 7 and line 17a may be the two-phonon (TO) line associated with line 8.

The second experiment involving InP:Yb examined the changing intensity pattern of all known Yb lines near 1 μm as a function of temperature and excitation energy. The goal of this line of research is to explore how the various emissions are affected by changing conditions, which may lead to a better understanding of the mechanism responsible for transferring incident energy into the Yb^{3+} ions. In all cases PMT temperature and bias, spectrometer speed, sample position and slit sizes remained the same. Excitation energies from 1.380 eV to 1.459 eV and temperatures from 2.8K to 90K were used in this study. For each excitation energy selected, data was taken at each of the indicated temperatures. The signal was optimized prior to each scan by making minor adjustments to the lens that focuses on the spectrometer slit. As the excitation energy decreased and as the temperature increased, the signals of all lines inevitably were extinguished.

Figure 19 graphically depicts the temperature dependence of selected lines at four different excitation energies, which cross the bandgap of InP (≈1.42 eV). Lines 2, 4, 8, 9, and 11 are the lines shown in this figure and were used due to their clarity in the spectra at most

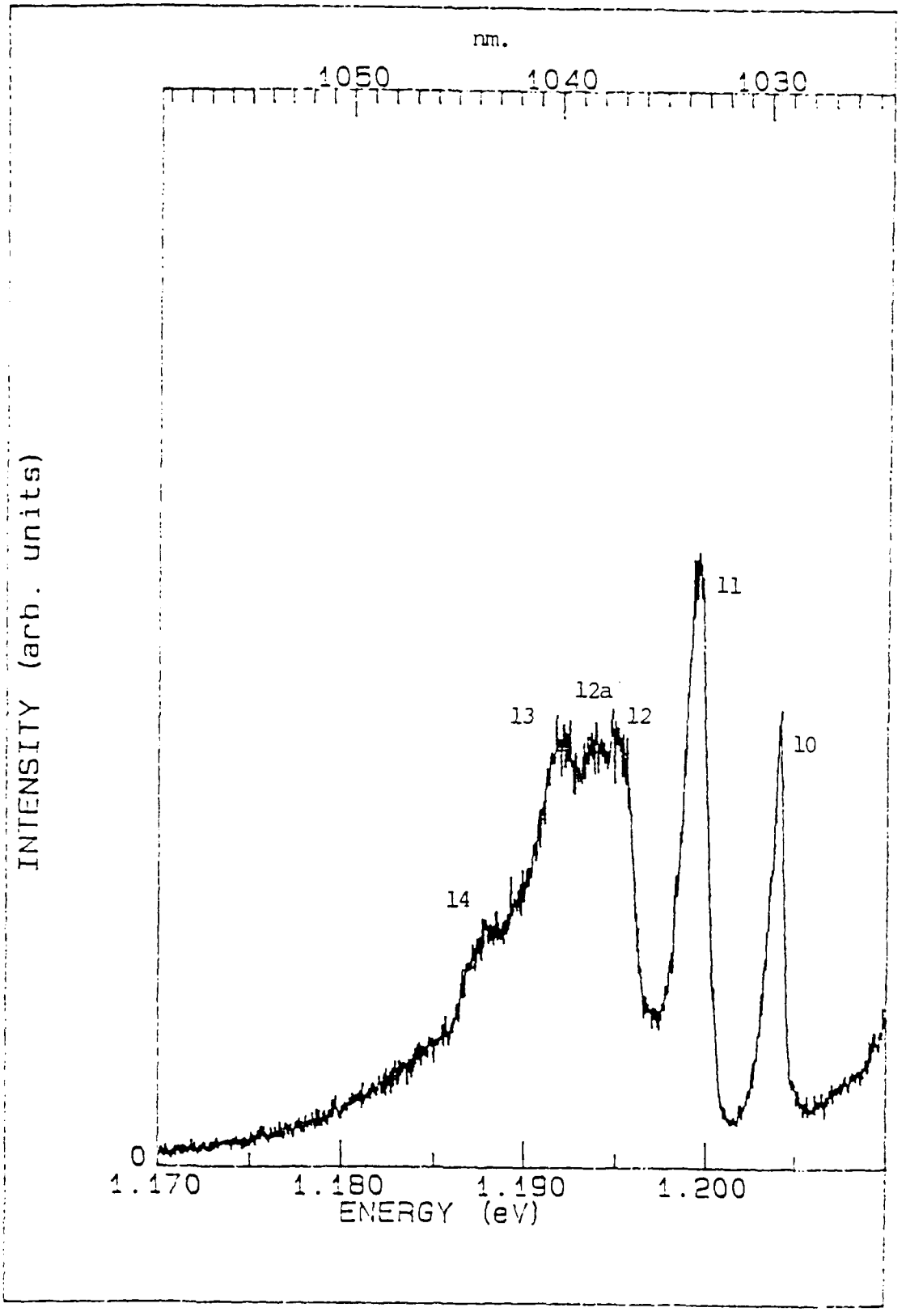

Figure 17. Evidence of Line 12a in PL Spectra of InP:Yb at 5.4 W/cm^2

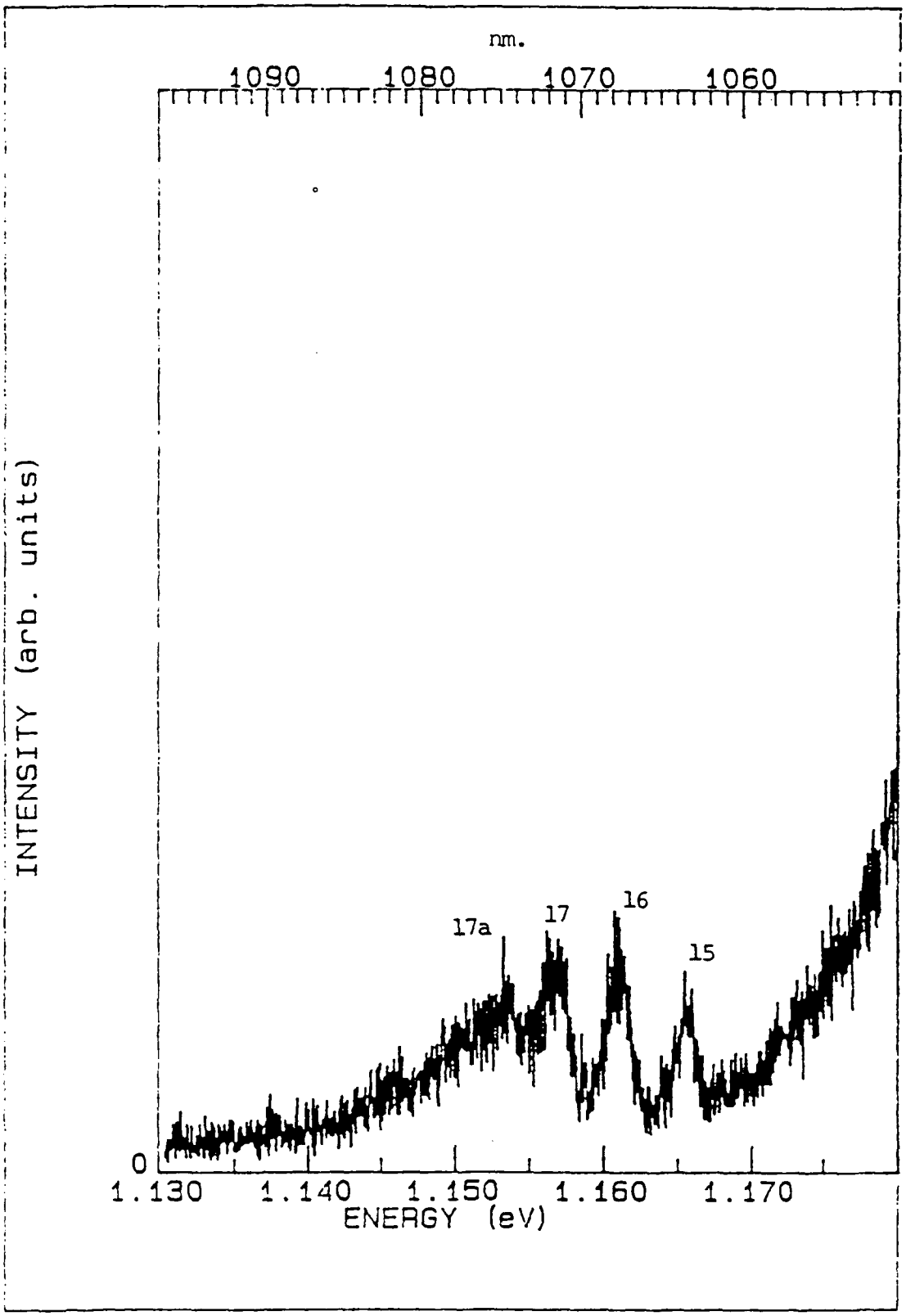

Figure 18. Evidence of Line 17a in PL Spectra of InP:Yb at 5.4 W/cm^2

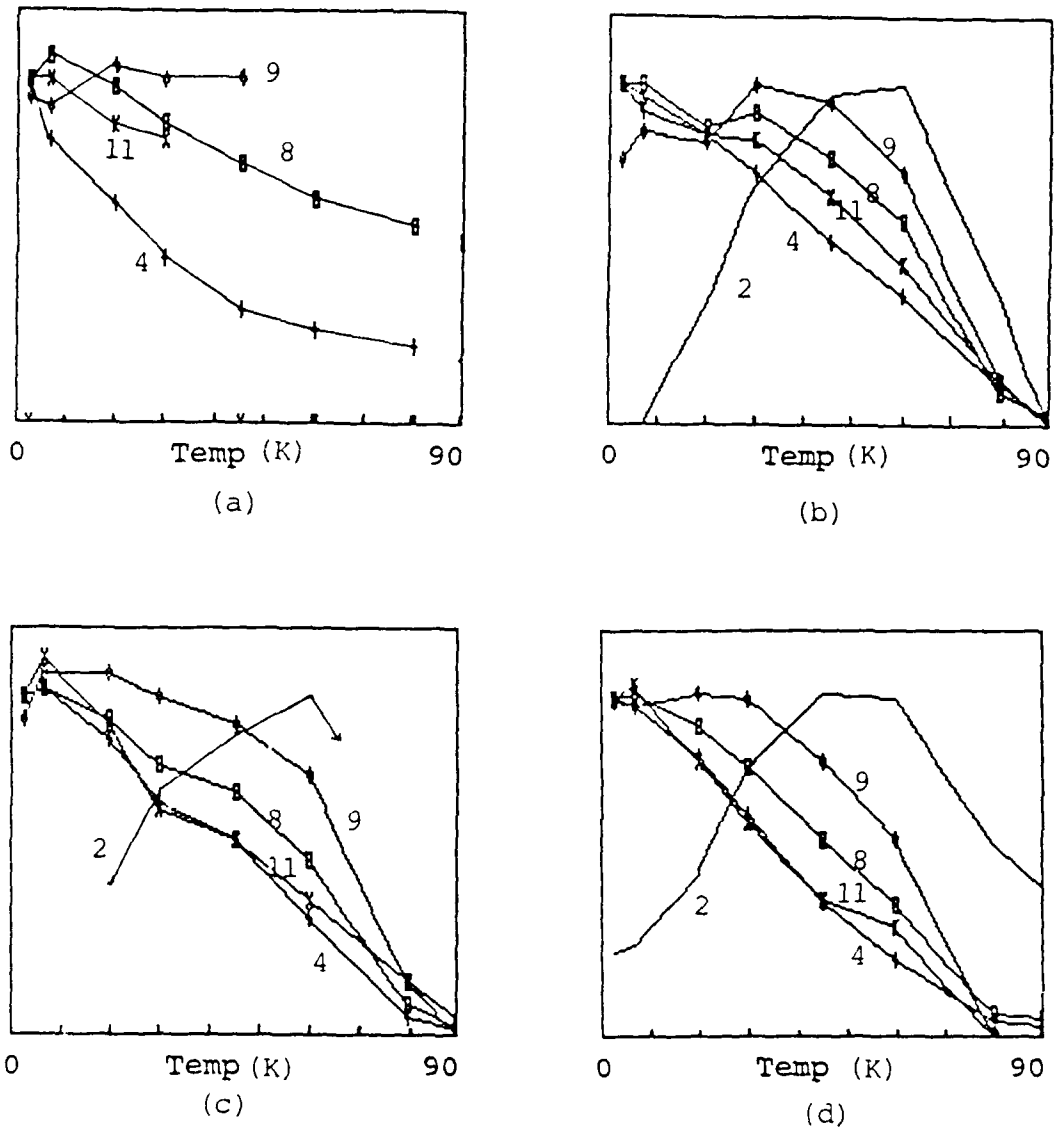

Figure 19. Temperature Dependence of Peak Intensities of Lines 2, 4, 8, 9, and 11 at Excitation Energies 1.4095 eV (a), 1.418 eV (b), 1.425 eV (c), and 1.459 eV (d). Vertical Scale is Intensity Normalized to One for Comparison.

excitation energies and temperatures. Line 3 could not be evaluated because even at moderate temperatures it became substantially influenced, and then masked, by line 4. At the lowest energy used in the figure, 1.4095 eV, line 2 could not be considered and only those points connected by a line can be considered as reliable values. In all of the figures, the value for line 2 at 80K and 90K must be considered with caution because the breadth of line 4 at those temperatures is sufficient to influence and possibly inflate the intensity of line 2. Finally, the intensity of the lines in all figures have been normalized to one to allow comparison of trends in intensities; for relative intensities, see Figure 5 or 15.

It is clear that the general trends indicated in Figure 19 are similar for each excitation energy. A brief qualitative argument will demonstrate how the data support the accepted line assignments and associated energy level diagram. First, after initially losing intensity as a function of temperature at the same rate as line 4, line 8 shows a slower rate of loss at the moderate temperatures (below ≈60K). This indicates that as the temperature rises, the probability of the transition from Γ_8 level of the excited state to the Γ_7 level of the spin orbit ground state increases compared to the transition indicated by line 4. Second, at the lowest temperatures the Γ_6 state of the $^2F_{5/2}$ upper spin orbit level is virtually unpopulated, but as the

temperature increases, thermal excitation dramatically increases the population of this state, increasing the probability of a line 2 transition (confirming the "hot line" characteristic mentioned earlier). Presumably, the transitions from this upper level to the Γ_7 and Γ_8 states of the ground spin orbit level are also enhanced but cannot be seen due to the strength of other lines.

Although there is no proposed explanation for the existence of line 9 (or 5, 6, or 7, for that matter), it is interesting to note its trends in Figure 19. It appears to have a "hot line" characteristic to a small degree and maintains a slower rate of intensity loss through the moderate temperatures. This would indicate that line 9 may be associated with upper crystal field split level transitions of the excited spin orbit state.

Figure 20 shows the intensity of the indicated lines as a function of excitation energy. The significance of these results is that there is a noticeable peak in intensity in all spectral lines at all evaluated temperatures. This peak occurs in all cases very near 1.42 eV which correlates with the InP band edge. At higher energies, the intensity is generally level at a value slightly below the peak intensity, while at excitation energies slightly below 1.42 eV there is a dramatic decrease in line intensity. Since all lines behave uniformly, this is further evidence that all lines of the Yb spectra are derived from the same

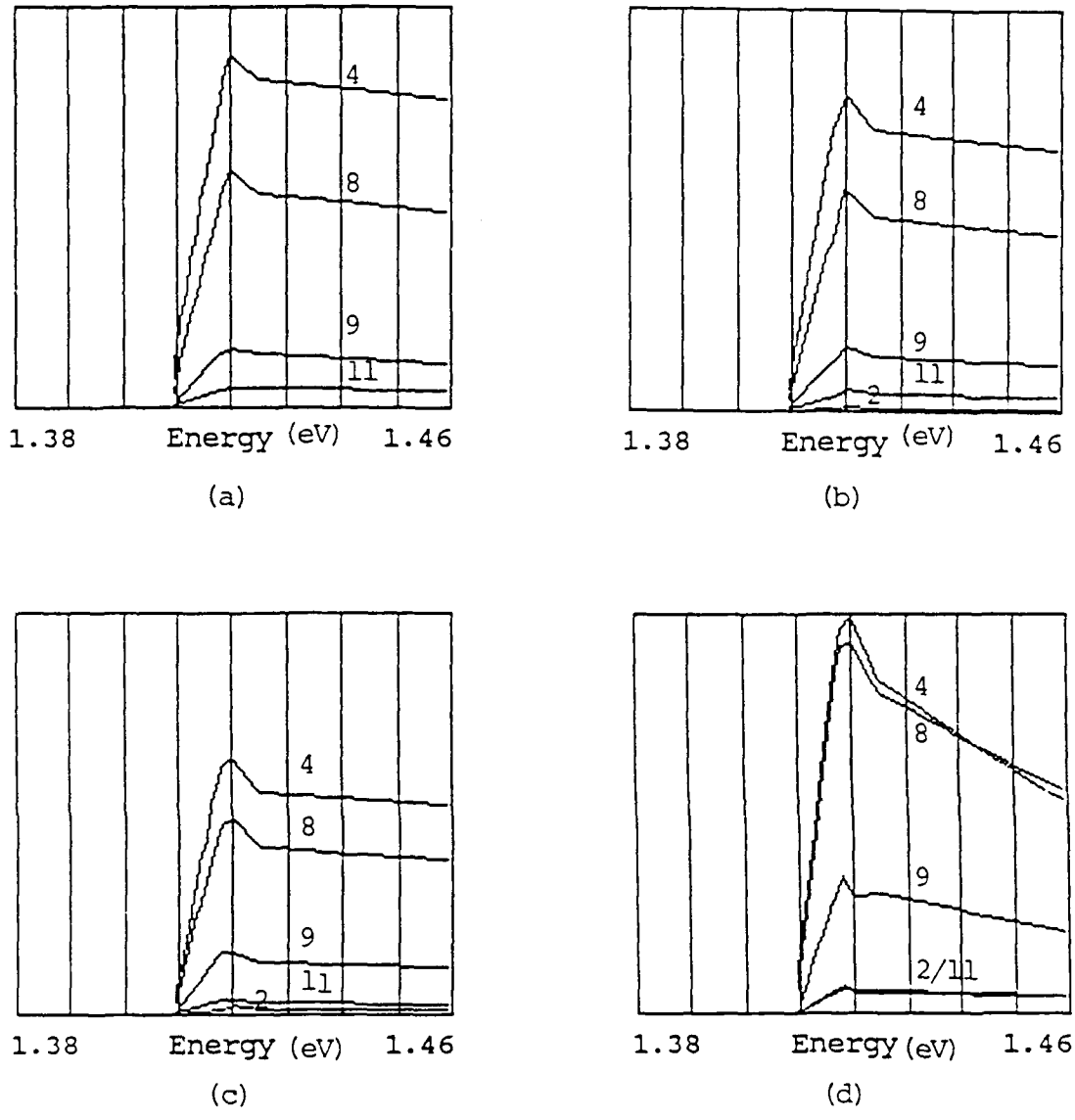

Figure 20. Energy Dependence of Intensities of Lines 2, 4, 8, 9, and 11 at Temperatures 7K (a), 20K (b), 30K (c), and 60K (d). Vertical Scale is Intensity of Arbitrary Units. Plot Maximum in (a), (b), and (c) is 3 x that in (d).

luminescent center. Furthermore, this phenomenon indicates that a resonance is occurring with the very near band gap transitions, implying that free carriers and probably excitons are most responsible for Yb 4f excitation. Note that as the excitation energy decreases toward the (D^o,A^o) region, the signal intensity is sharply reduced and at the lowest energy, 1.38 eV, which is very near the D-A peak, there is still no rise in intensity. Although equipment limitations prevented excitation with energy below 1.38 eV, the results imply that donor-acceptor pairs in the material do not have a significant role in Yb excitation.

Yb Implanted VPE InP

An SEL investigation was accomplished on a n-type VPE InP sample that was implanted at 1 MeV with 3 x 10^{13} Yb^{3+} ions/cm^2 and annealed at 550°C for 15 sec using RTA. Although the Yb emissions from this sample were not as strong as those for the bulk grown InP, this sample also exhibited near band edge and donor-acceptor spectra that were not seen in the bulk InP:Yb. With this sample the near band edge transitions were excited and both the (D^o,A^o) and the Yb luminescence were evaluated. The 2.5 W/cm^2 PL spectra taken at 7K is shown in Figure 21. Excitonic transitions near 1.418 eV, free to bound and (D^o,A^o) transitions near 1.371 eV, and two transitions possibly associated with deep donors or acceptors near 1.305 eV can

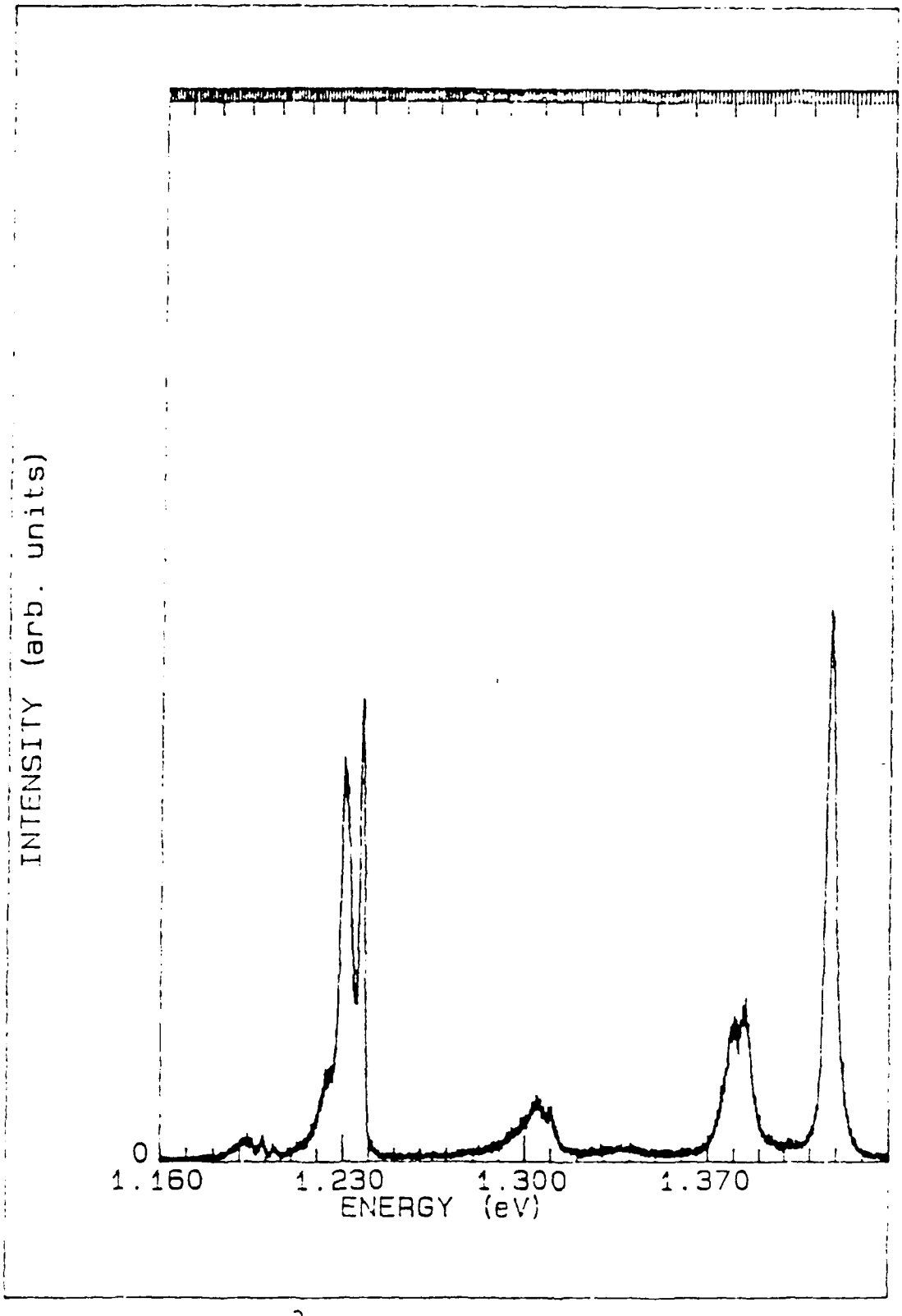

Figure 21. 2.5 W/cm^2 PL Spectra of VPE InP:Yb. Temperature = 7K.

be seen in this figure in addition to Yb lines 4 and 8 near 1.23 eV. Figure 22 shows the 160 mW/cm^2 (10 mW total power) spectra at three selected excitation energies. Note that the spectra with the lowest free to bound and (D^o,A^o) intensity was obtained at an energy between the energies used to obtain the upper two curves. This will be more thoroughly discussed in the following paragraphs.

Figure 23 is a compilation of the findings in this study. Excitation energies from 1.4162 eV to 1.4214 eV were used at 10 mW. In this range it is clear that the (D^o,A^o) transitions experience a significant dip in intensity. It is also clear that the Yb emissions increase slightly over the region in which the (D^o,A^o) transitions dip and actually reach a peak at the same energy at which the D-A emission reaches a low. Several physical and experimental-related possibilities are offered in the following paragraphs.

The lack of smoothness and consistency of the lines in figure 23 suggests that experimental error may have been a factor. The primary source of error in this experiment was in the setting of 10 mW of incident power at each energy change. The instrument error involved with reading the Coherent power meter was ± .5 mW which, from earlier calculations, is sufficient to induce approximately 5.5% error in the intensity readings. This error added to any other smaller errors can be responsible for the roughness of the lines but not for the general trends.

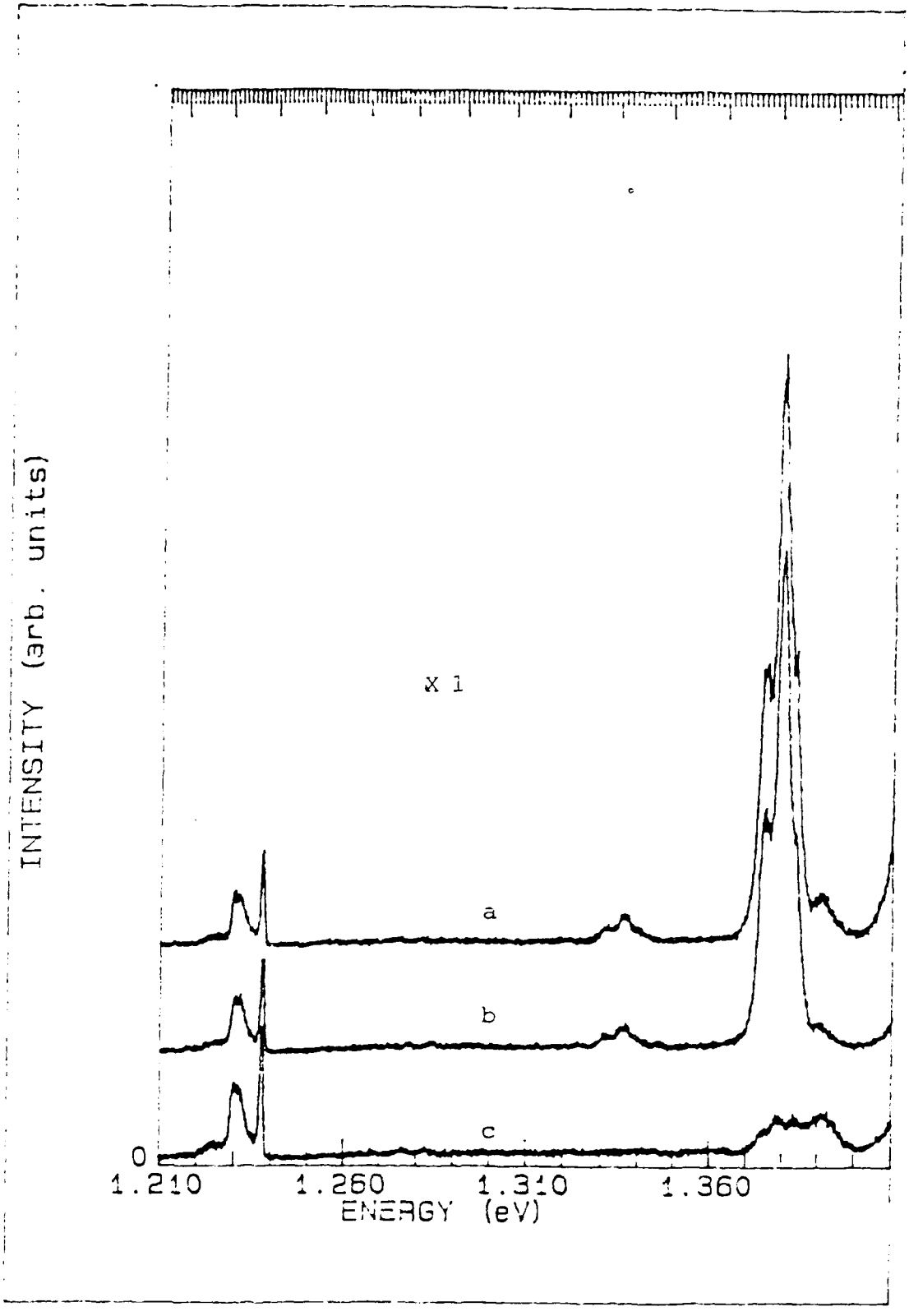

Figure 22. SEL Spectra of VPE InP:Yb at 1.4170 eV (a), 1.4207 eV (b), and 1.4186 eV (c). Irradiance = 0.16 W/cm^2.

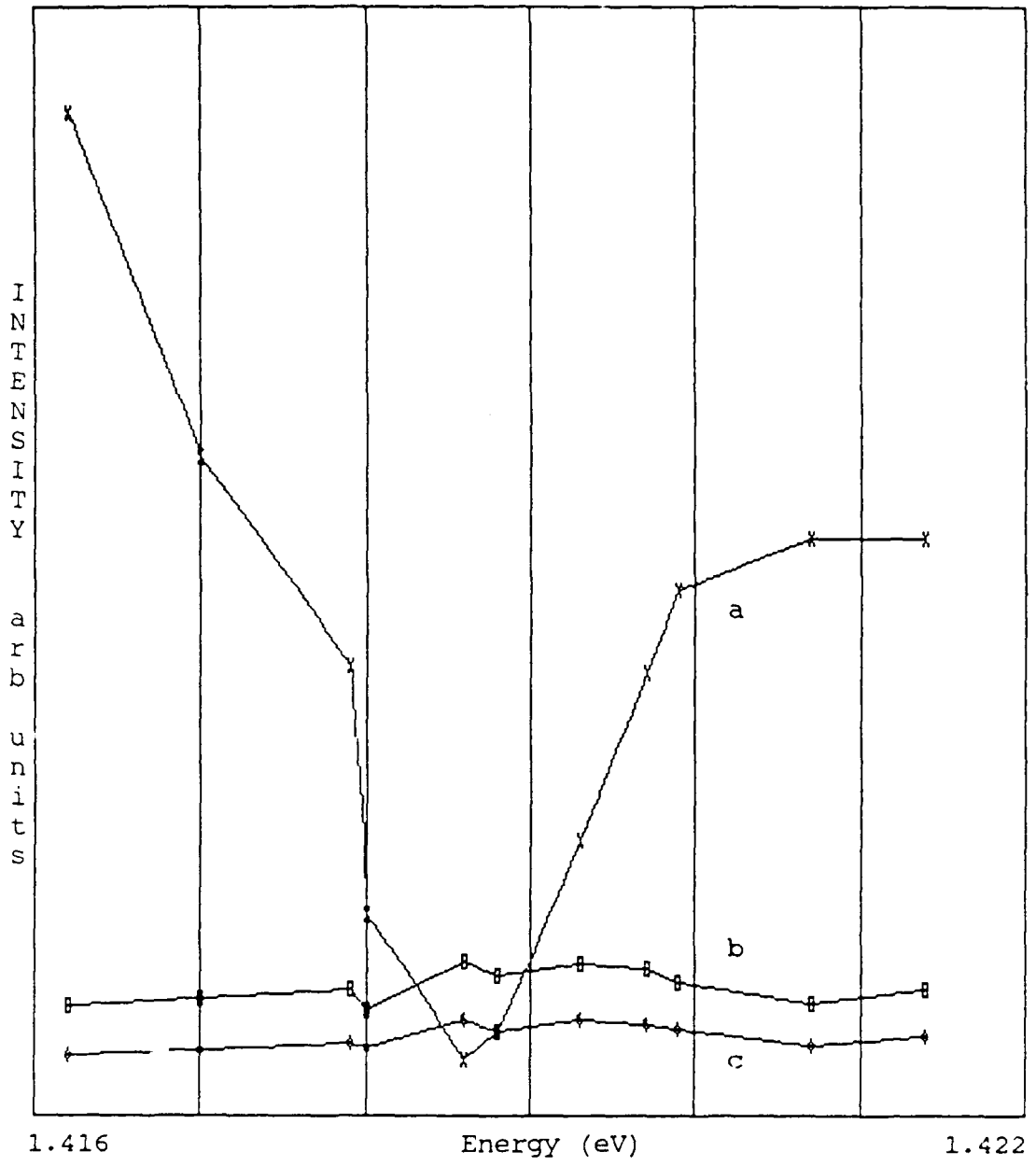

Figure 23. Excitation Energy Dependence of Donor-Acceptor Pair Transitions (a), Line 4 (b), and Line 8 (c). Sample Temperature for Experiment = 7K.

The dip in the donor-acceptor curve represents a decrease of about 90% from its value at 1.4207 eV while the peak in the Yb emission represents an increase of about 36% from its value at the same energy. It is also apparent from Figure 23 that there is only a small change in the Yb signal for substantial changes in the (D^o,A^o) emissions. Therefore, it seems that if the donor-acceptor transitions do play a role in the transfer of excitation energy to the Yb ions, then it must be a fairly minor role with a low efficiency of energy transfer.

It is important to note that the selected energy range corresponds to the approximate exciton emission energies for the material as seen in Figure 21 and that the Yb peak and (D^o,A^o) dip occur at the excitation laser energy precisely equivalent to the peak of the exciton emission. This supports the theory that excitons and/or free carriers are most responsible for the transmission of energy to the Yb ions, particularly since they seem to avoid exciting the donor-acceptor pairs when they are in resonance with the incoming excitation photons.

Yb Implanted GaAs and AlGaAs

Many samples of both GaAs and AlGaAs doped with Yb were examined using PL techniques. Although characteristic Yb signals have been reported in the literature (16, 18, 23), none of the samples examined here demonstrated Yb luminescence. Table 1 lists the GaAs and AlGaAs samples

that were studied along with each sample's anneal temperature. Many of the samples were annealed again (as indicated in Table 1) in an attempt to locate Yb emissions. All samples were doped at a dosage of $3x10^{13}$ $ions/cm^3$ with an implantation energy of 1 MeV. The last column of the table indicates whether the particular samples had displayed Yb emissions in previous research conducted by Jose Colon (24). It is important to note that signals found in Colon's investigation were extremely weak and were found on an experimental setup similar to that in this current research. The following paragraphs delineate a possible explanation for lack of Yb signal in the GaAs and AlGaAs samples.

As indicated earlier, Kozanecki and Gröetzschel published research results on the location of Yb in GaP and GaAs lattices (13). Their use of Rutherford backscattering (RBS) and $^4He^+$ ion channeling measurements on Yb implanted GaP and GaAs resulted in strong evidence that the majority of the Yb atoms reside at nonsubstitutional positions and that they diffuse to the surface with subsequent annealing (13).

Kasatkin had published a study on the instability of low symmetry Yb^{3+} luminescent centers in GaP. In that report he states, "...storage in darkness under normal conditions reduced the integrated intensity of the luminescence emitted by all the low-symmetry Yb^{3+} centers."(29) He emphasizes that after prolonged storage

Table 1
GaAs and AlGaAs Samples Examined.

Substrate	Anneal Method/Temp(°C)/Time	Yb Emissions Previously Observed
s.i. GaAs	CFA/650/15 min	yes
	Reanneal CFA/700/10 min	X
"	CFA/640/10 min	?
	Reanneal CFA/675/10 min	X
"	RTA/500/12 sec + CFA/640/10 min	?
"	RTA/975/15 sec + RTA/500/15 sec	no
	Reanneal CFA/700/10 min	X
"	RTA/900/12 sec + RTA/950/15 sec	?
	Reanneal CFA/675/10 min	X
n- GaAs	CFA/650/15 min	yes
	Reanneal CFA/675/10 min	X
"	RTA/900/12 sec + RTA/950/15 sec	?
	Reanneal CFA/700/10 min	X
"	RTA/600/12 sec	no
"	RTA/700/12 sec	no
"	RTA/500/12 sec	no
p- GaAs	RTA/600/12 sec	no
"	RTA/900/12 sec + RTA/950/15 sec	?
n- VPE GaAs	CFA/650/15 min	?
"	RTA/975/15 sec + RTA/500/15 sec	?
$Al_{.30}Ga_{.70}As$	RTA/950/15 sec	yes
"	RTA/800/12 sec	yes

Table 1 (continued)

$Al_{.23}Ga_{.77}As$	RTA/800/15 sec	yes
"	RTA/975/15 sec + RTA 500/15 sec	no
$Al_{.15}Ga_{.85}As$	RTA/975/15 sec + RTA/500/15 sec	yes

key to table:

yes--Yb related signals were identified by Colon

no---Yb related signals were not found by Colon

?----results of experiment are unknown

X----experiments have not yet been conducted

GaP:Yb exhibited only the Yb centers associated with T_d symmetry and had lost the emissions associated with low symmetry. Annealing also eliminated low symmetry emissions.

In light of these and other experiments discussed earlier it seems probable that Yb implantation into GaAs and AlGaAs crystals may take place primarily on low symmetry interstitial sites and form a variety of complexes that are sample dependent. It also seems likely that prolonged storage (on the order of a year or more for all samples in Table 1) and annealing have reduced the initial signal to one undetectable by the current setup.

Conclusions and Recommendations

The results of the experiments confirm several theories concerning the structure of the energy level diagram for InP:Yb. First, the indication that all but one line of the Yb emission have the same energy dependence reconfirms that the lines come from only one luminescent center. Second, the energy level diagram matches very well not only with the theoretical calculations from which it was derived but also with the experimental results as shown in this and other research. Third, the "hot line" nature of line 2 was verified, showing convincingly that the transition must initiate at the upper crystal field split Γ_6 level of the $^2F_{5/2}$ state. Fourth, the results strongly support the phonon replica explanation for lines 10-17.

The results also add credence to one of the excitation mechanism theories. The fact that Yb emissions reach peak intensity when the sample is excited in the exciton absorption region is a strong indication that excitons and/or free carriers play a crucial role in the transfer of energy to the Yb ions. While the results also indicate that there may be some correlation between the donor-acceptor emissions and the Yb related spectrum, they are not convincing since the change in Yb emissions are so small relative to the change in (D^o,A^o) luminescence.

The results for GaAs and AlGaAs were somewhat

disappointing in that they did not allow the intended selective excitation study; however, much was also learned from the lack of signals. It is probable that the implanted Yb ions reside on interstitial sites in these materials and that the weak signals previously reported were quenched by extended storage and repeated annealing. Considerable research can be accomplished to analyze the processes involved in the signal quenching and studies can be undertaken to reduce the effect. It is clear however that SEL measurements will be impractical until a sample with strong Yb emissions is obtained.

My suggestions for further study of InP:Yb include obtaining a solid state tunable laser that will allow one to excite over a wider range of energies than with the system currently available. PLE techniques could then be used to monitor the Yb emissions as a function of excitation energy which will convincingly support one of the three excitation transfer mechanisms proposed by previous researchers. Codoping InP:Yb could also be an exciting avenue of research in the quest for sharp but intense emissions at room temperature.

Finally, future research projects should include the use of SEL and PLE to study the energy level structure and excitation mechanisms of the whole gamut of RE doped III-V semiconductors. Since a relatively strong signal is necessary for extensive energy and temperature studies as

accomplished in this current study, any SEL or PLE proposed experiment should be based on results of a previously accomplished optimization study using PL techniques.

The Air Force's interest in this line of research is evident. The excitation mechanisms behind the superior signals from RE doped III-V semiconductors will probably be well understood in the near future; this understanding will open the doors to faster, less expensive, and more reliable communications systems. In order to be in the forefront of this burgeoning technology, this service must continue to pursue the elusive energy transfer mechanisms.

Bibliography

1. Aszodi, G. et al. "Zeeman Analysis of the Ytterbium Luminescence in Indium Phosphide," Physical Review B, 31 (1985).

2. Haydl, W. H. et al. "Ytterbium-doped InP Light Emitting Diode at 1 μm," Applied Physics Letters, 46(9) (May 1985).

3. Tsang, W. T. "Observation of Enhanced Single Longitudinal Mode Operation in 1.5 μm GaInAsP Erbium Doped Semiconductor Injection Lasers," Applied Physics Letters, 49(25) (December 2986)

4. Kasatkin, V. A. et al. "Intracenter Transitions in Yb^{3+} Impurities in Gallium Phosphide," Soviet Physics Semiconductor, 14(9) (September 1980).

5. Zakharenkov, L. F. et al. "Photoluminescence of Epitaxial InP:Yb Films," Soviet Physics Semiconductor, 15(8) (August 1981).

6. McKelvy, J. P. Solid State and Semiconductor Physics. Malabar, Florida: Robert E. Krieger Publishing Company, 1986.

7. Matarè, H. G. Defect Electronics in Semiconductors. New York: Wiley-Interscience, 1971.

8. Lumb, M. D. Luminescence Spectroscopy. London: Academic Press, 1978.

9. Pankove, J. I. Optical Processes in Semiconductors. New York: Dover Publications, 1975.

10. Streetman, B. G. Solid State Electronic Devices. Englewood Cliffs, New Jersey: Prentice Hall, Inc., 1984.

11. Mayer, J. W. et al. Ion Implantation. New York: Academic Press, 1970.

12. Ermakov, L. K. et al. "Luminescence of Ytterbium in Gallium and Indium Phosphides," Optical Spectroscopy (USSR), 57(1) (July 1984).

13. Kozanecki, A. and R. Gröetzschel, "On the Location of Ytterbium in GaP and GaAs Lattices," Journal of Applied Physics, 64(6) (September 1988).

14. Masterov, V. F. "Paramagnetic Resonance and Relaxation of Trivalent Ytterbium in Indium Phosphide," Soviet Physics Solid State, 25(5) (May 1983).

15. Wybourne, B. J. Spectroscopy Properties of Rare Earths. New York: Interscience Publishers, 1965.

16. Ennen, H. et al. "Luminescence of the Rare Earth Ion Ytterbium in InP, GaP, and GaAs," Journal of Applied Physics, 57(6) (March 1985).

17. Koster, G. F. et al. Properties of the Thirty Two Point Groups. Cambridge, Massachusetts: M.I.T. Press, 1963.

18. Ennen, H. and J. Schneider. "Luminescence of Rare Earth Ions in III-V Semiconductors," Proceedings of the Thirteenth International Conference on Defects in Semiconductors, 115-127 (August 1984).

19. Klein, P. B. "Time Resolved Photoluminescence from Yb^{3+}," Solid State Communications, 65(10) (1988).

20. Hemstreet, L. A. "The Electronic States of a substitutional Ytterbium Impurity in Indium Phosphide," Materials Science Forum, edited by H. J. von Bardeleben (Trans Tech Publication Aedurmannsdor, Switzerland) vol 10-12, 85-90 (1986).

21. Raczynska, J. "Donor Gettering in GaAs by Rare Earth Elements," Applied Physics Letters 53(9) (August 1988).

22. Nakagome, N. et al. "Liquid Phase Epitaxy and Characterization of Rare Earth Ion (Yb, Er) Doped InP," Journal of Crystal Growth 85: 345-356 (1987).

23. Gippius, A. A. "Defects and Optically Active Transition and Rare Earth Elements in III-V and II-VI Semiconductors and Diamond," Defects in Semiconductors, edited by H. J. von Bardeleben. Material Science Forum Vols 10 -12 (1986).

24. Colon, Jose E. Low Temperature Photoluminescence Study of Ytterbium Implanted into III-V Semiconductors and AlGaAs. MS thesis, AFIT/GET/88D. School of Engineering, Air Force Institute of Technology (AU), Wright Patterson AFB OH, December 1988.

25. Wagner, J. et al. "Photoluminescence Excitation Spectroscopy on InP:Yb," Physical Review B, 30(10) (November 1984).

26. Kasatkin, V. A. and V. P. Savel'ev. "Excitation of Ytterbium Luminescence in Gallium and Indium Phosphides,"

Soviet Physics Semiconductor, 18(9) (September 1984).

27. Kasatkin, V. A. et al. "Kinetics of the Electroluminescence of Ytterbium Ions in Indium Phosphide," Soviet Physics Semiconductor, 19(2) (February 1985).

28. Körber, W. and A. Hangleiter, "Excitation and Decay Mechanisms of the Intra 4f Luminescence of Yb^{3+} in Epitaxial InP:Yb Layers," Applied Physics Letters, 52(2) (January 1988).

29. Kasatkin, V. A. "Instability of Low Symmetry Yb^{3+} and Pr^{3+} Luminescence Centers in Gallium Phosphide," Soviet Physics Semiconductor, 19(10) (October 1985).

Vita

Capt Michael L. Eastman [redacted] into an Air Force family. He graduated from Holliday High School in Holliday, Texas, in 1976. Four years later he graduated from the Air Force Academy with a Bachelor of Science in Electrical Engineering.

Capt Eastman began his Air Force career in pilot training and then as a T-38 instructor pilot at Reese AFB, Texas. He followed that assignment with one to Dover AFB, Delaware as a C-5 flight examiner aircraft commander. He entered the Air Force Institute of Technology at Wright-Patterson AFB, Ohio, in 1988, to pursue a Master of Science in Engineering Physics.

[redacted]

SECURITY CLASSIFICATION OF THIS PAGE

REPORT DOCUMENTATION PAGE

Form Approved
OMB No. 0704-0188

1a. REPORT SECURITY CLASSIFICATION UNCLASSIFIED	1b. RESTRICTIVE MARKINGS
2a. SECURITY CLASSIFICATION AUTHORITY	3. DISTRIBUTION / AVAILABILITY OF REPORT APPROVED FOR PUBLIC RELEASE; DISTRIBUTION UNLIMITED
2b. DECLASSIFICATION / DOWNGRADING SCHEDULE	
4. PERFORMING ORGANIZATION REPORT NUMBER(S) AFIT/GEP/ENP/89D-3	5. MONITORING ORGANIZATION REPORT NUMBER(S)
6a. NAME OF PERFORMING ORGANIZATION SCHOOL OF ENGINEERING 6b. OFFICE SYMBOL (If applicable) AFIT/ENP	7a. NAME OF MONITORING ORGANIZATION
6c. ADDRESS (City, State, and ZIP Code) AIR FORCE INSTITUTE OF TECHNOLOGY (AU) WRIGHT-PATTERSON AFBOH 45433-6583	7b. ADDRESS (City, State, and ZIP Code)
8a. NAME OF FUNDING / SPONSORING ORGANIZATION 8b. OFFICE SYMBOL (If applicable)	9. PROCUREMENT INSTRUMENT IDENTIFICATION NUMBER
8c. ADDRESS (City, State, and ZIP Code)	10. SOURCE OF FUNDING NUMBERS PROGRAM ELEMENT NO. / PROJECT NO. / TASK NO / WORK UNIT ACCESSION NO.

11. TITLE (Include Security Classification)
SELECTIVE EXCITATION LUMINESCENCE AND PHOTOLUMINESCENCE INVESTIGATIONS OF YTTERBIUM DOPED InP, GaAs, and AlGaAs

12. PERSONAL AUTHOR(S)
EASTMAN, MICHAEL L., CAPT, USAF

13a. TYPE OF REPORT	13b. TIME COVERED	14. DATE OF REPORT (Year, Month, Day)	15. PAGE COUNT
MS THESIS	FROM _____ TO _____	1989 DECEMBER	82

16. SUPPLEMENTARY NOTATION

17. COSATI CODES			18. SUBJECT TERMS (Continue on reverse if necessary and identify by block number)
FIELD	GROUP	SUB-GROUP	
07	02		PHOTOLUMINESCENCE, YTTERBIUM
20	05		GALLIUM ARSENIDES, INDIUM PHOSPHIDES

19. ABSTRACT (Continue on reverse if necessary and identify by block number)

THESIS ADVISOR: YUNG KEE YEO, PhD
ASSOCIATE PROFESSOR OF PHYSICS

20. DISTRIBUTION / AVAILABILITY OF ABSTRACT ☒ UNCLASSIFIED / UNLIMITED ☐ SAME AS RPT ☐ DTIC USERS	21. ABSTRACT SECURITY CLASSIFICATION UNCLASSIFIED
22a. NAME OF RESPONSIBLE INDIVIDUAL YUNG KEE YEO, PhD	22b. TELEPHONE (Include Area Code) (513) 255-2012 22c. OFFICE SYMBOL AFIT/ENP

DD Form 1473, JUN 86 Previous editions are obsolete SECURITY CLASSIFICATION OF THIS PAGE

UNCLASSIFIED

Abstract

Group III-V semiconductors doped with rare earth (RE) elements produce sharp emissions that would be ideally suited to Air Force optoelectronic applications. The sharp emissions are due to the intra-4f transitions of the triply ionized RE atom that are partially shielded from the crystal lattice potential by the outer lying 5s and 5p electrons. In this work the RE element ytterbium (Yb) was implanted into bulk grown InP, vapor phase epitaxial (VPE) grown InP, GaAs, and $Al_xGa_{1-x}As$ with x = .15, .23 and .30. The Yb was implanted at 1 MeV at a dosage of $3 \times 10^{13}/cm^2$. The samples were annealed using rapid thermal annealing (RTA) or conventional furnace annealing (CFA) for a range of temperatures and times.

The study of bulk InP:Yb evaluated the emission spectra intensity as a function of temperature and excitation energy. Temperatures from 2.8K to 90K and energies from 1.38 eV to 1.495 eV were used. The results of this analysis confirm that the majority of the Yb related spectra is from only one luminescent center. They also illustrate a definite peak in emission intensity at excitation energies that correlate to the excitonic absorption region of the semiconductor. This indicates that the excitons and/or free carriers are required for the transfer of energy to the Yb ions. An incident power versus line intensity study was also accomplished. Results indicate most lines saturate at higher powers but the 1.248 eV line (line 2) increases significantly, possibly as a result of its "hot line" characteristic.

The study of VPE InP:Yb involved excitation over a narrow range that corresponds to the band edge. Donor-acceptor (D^o,A^o) pair transitions were monitored as well as Yb emissions. Results showed a substantial dip in the (D^o,A^o) emissions with a simultaneous minor peak in the Yb signal. Although this seems to indicate a possible link between (D^o,A^o) transfer of energy to Yb, the slight change in Yb intensity indicates that if this is a transfer method, it is extremely inefficient.

The photoluminescence of many GaAs:Yb and AlGaAs:Yb samples were examined but no characteristic Yb emissions were found. Some of the samples had previously been studied and had exhibited very weak Yb related signals. The possibility of signal quenching by storage and annealing is proposed.